USING HANSEN SOLUBILITY PARAMETERS (HSPS) TO DEVELOP ANTIOXIDANT-PACKAGING FILM TO ACHIEVE CONTROLLED RELEASE

By

Jing Gao

A THESIS

Submitted to
Michigan State University
in partial fulfillment of the requirements
for the degree of

Packaging-Master of Science

2014

ABSTRACT

USING HANSEN SOLUBILITY PARAMETERS (HSPs) TO DEVELOP ANTIOXIDANT-PACKAGING FILM TO ACHIEVE CONTROLLED RELEASE

By

Jing Gao

The Hansen Solubility Parameters (HSPs) methodology was used to estimate the affinity between poly (butylene adipate-*co*-terephthalate) (PBAT) and 25 commonly used antioxidants. The HSPs of PBAT and the antioxidants were calculated by the Hoftyzer and Van Krevelen group contributions method, and the HSPs of PBAT were also experimentally determined. The HSPs of PBAT were δ_d =18.97 ± 0.30, δ_p =4.83 ± 0.75 and δ_h =9.10 ± 0.30. Of the selected 25 antioxidants, two antioxidants-α-tocopherol (α-TOC) and propyl gallate (PG), were incorporated into the PBAT matrix according to their likelihood to migrate from PBAT. Migration test at 10, 20, and 30℃ from the produced antioxidant films (α-TOC-PBAT (PBA) and PG-PBAT (PBP)) into 95% ethanol were conducted to verify the initial migration estimation. The Fick's diffusion equations were used to estimate the diffusion coefficients (*D*) and the mass of antioxidants release at equilibrium (M_∞). The partition coefficients ($K_{P,S}$) were determined from the M_∞. *D* values obtained at all three temperatures for the two films were of the same order of magnitude (10^{-9} cm^2/s) indicating a very fast release of α-TOC and PG from PBAT. Due to the fast release of the antioxidants from PBAT, the HSP method was not able to properly predict the likelihood of α-TOC and PG migration from the PBAT films. The activation energy (*Ea*) was determined by the Arrhenius equation, as 48.5kJ/mol for PBA film and 54.4kJ/mol for PBP film. The optical properties of PBA and PBP films are also reported in this study.

ACKNOWLEDGMENTS

First of all, I would like to give my precious appreciation to my major advisor, Dr. Rafael Auras for accepting me in to his research group and giving me the opportunity to work on this interesting project. As my advisor, he gave me many guidance and valuable suggestions on my experiment and thesis writing. I appreciate his patient and encouragement, making me brave to finish my research. I appreciate his tolerant heart on the mistakes I made in my research. I also appreciate his educational and professional support for many books and articles he offered me. Thank you very much for Dr. Auras. I would not finish this project without your mentoring.

I would like to thank my committee members Dr. Maria Rubino and Dr. Kirk Dolan for their kindly guidance and support throughout my projects. I am very thankful to Aaron Walworth and Ajay Kathuria for training and helping me in all the machines that I have used for my research purpose in school of packaging at MSU. I would like to thank Dr. Daniel Jones and Dr. Jiangyin Bao from the department of Biochemistry & Molecular Biology for their assistance with my Mass Spectrometry analysis. I would also like to thank all the professors and advisors from School of Packaging, thank them for spreading the useful knowledge and organizing the interesting seminars. I really learned a lot during my master study.

I would like to convert my gratitude to all RAA research group members: Hayati, Kang, Ajay, Turk, Sukkeewan, Fabiola, Edgar, Saleh, Soohyung, Javiera, Marcelo, Rodolfo, Ning, Siyuan for their kindness and timely assistance and sharing the invaluable expertise with me. A special thanks to Hayati for sharing her knowledge and being a great guidance in migration modeling analysis. Without her help, I could not easily analyze my migration data. I would also like to thank Yining Xia for our discussion about my project and Saleh for his help in the

statistical analysis of the results. Not to forget, Rijosh John Cheruvathur, thank you very much for your support on my film process.

I could not thank enough to all my friends for their encouragement and kindness. It is a magic that we met each other. And it will be a great memory in my life that we share the happiness and sorrow together.

Last but not least, I would like to express my endless thanks to my dear parents, my brothers and my sisters. Thank you for your concerns and trust. I am extremely grateful for your support during my entire master's year. You are always in my heart.

Jing Gao

July, 2014

TABLE OF CONTENTS

LIST OF TABLES

LIST OF FIGURES

KEY TO SYMBOLS AND ABBREVIATIONS

AOx	Antioxidants
APF	Antioxidant packaging film
HSPs	Hansen solubility parameters
MAP	Modified atmosphere packaging
PG	Propyl gallate
OG	Octyl gallate
BHA	Butylhydroxyanisole
TBHQ	Tert-Butyl-hydroquinone
α-TOC	α-tocopherols
AA	Ascorbic acid
IR 1076	Irganox 1076
BHT	Butylated hydroxytoluene
PBAT	Poly (butylene adipate-*co*-terephthalate)
PBCM	PBAT without antioxidants control master batch
PBAM	α-TOC of PBAT master batch
PBPM	PG of PBAT master batch
PBC	PBAT control film
PBA	α-TOC of PBAT film
PBP	PG of PBAT film
D	Diffusion coefficient
C	Permeant concentration
t	Diffusion time

T_g	Glass transition temperature
E_a	Activation energy
R	Gas constant
T	Absolute temperature
C_s	Migrant concentration in the food or food simulant
$M_{s,t}$	Migration level at time t
$C_{P,0}$	Initial migrant concentration
L_P	Polymer film thickness
V_P	Volume of the polymer
V_s	Volume of the food or food simulant
$K_{P,s}$	Partition coefficient of the migrant
$M_{s,\infty}$	Migration level at equilibrium
A	Area of the polymer in contact with the food simulant
$RMSE$	Root mean-square error
R_a	Solubility parameter distance
δ_D	Dispersion parameter
δ_P	Polar parameter
δ_H	Hydrogen bonding parameter

CHAPTER 1 INTRODUCTION & MOTIVATION

1.1 Introduction

In the food industry, packaging plays a vital role to protect the products from the outer environment and to extend their shelf life. There are also other functions performed by a package like containment of the products and providing detailed information about the package about the products [1]. Still, for food products quality assurance is one of the most important functions of the package. For oxygen-sensitive foods like milk and other dairy products containing protein and lipid, which are subjected to oxidation and will generate oxidative rancidity when they are exposure to oxygen, then packages play an important role to delay and/or avoid oxygen exposure. Oxidative rancidity is a major cause of food quality deterioration, leading to the formation of undesirable off-flavors as well as unhealthful compounds [2, 3]. Thus, oxidized food products have decreasing acceptability by consumers. Several methods are developed to retard oxidation based on directly protecting the food by adding antioxidant and/or using the packaging system to delay oxygen permeation and/or releasing antioxidants. Antioxidants can inhibit the oxidation of foods by scavenging free radicals, chelating pro-oxidative metals and quenching singlet oxygen [4, 5]. They can be added to the food and/or the packaging system. If added to the food products, they are highly effective; but their type and amount are highly regulated by the United States Food Drug Administration (FDA) and other international agencies to assure human's health [6]. The other method, and the subject of this thesis, is introducing the antioxidants on the packaging system for slow release. This method provides the advantage of controlling the amount of antioxidant releasing to the product in function of time, but it also provides a number of challenges such as degradation temperature, release kinetic control, and antioxidant stability.

Additionally methods used to delay oxygen intake are the use of oxygen scavenger in form of sachets that contains a compounds to scavenge the oxygen through oxidation reactions. These sachets are placed into the package together with the products. Some disadvantages of the sachets are the need for an additional packaging operation to add the sachet to the package, and the limit oxygen scavenger capacity of the sachet.

Antioxidant active packaging made as compounded polymeric membranes based on a polymer matrix and the addition of one or more antioxidants to control the release of the antioxidants in contact with the food has gaining attention as a feasible option to control food products' oxidation. The use of antioxidant polymeric membranes benefits both the packaging and the food products themselves because the addition of the antioxidant in the polymeric packaging may help to stabilize the polymer during processing and also favors to inhibit the products' oxidation [7-9]

Of the produced antioxidant polymeric films most of them are based on the use of commercial polymers such as polyolefins and/or polyester. Due to environmental concerns, a current trend is to develop APF made from biodegradable polymers and natural antioxidants. Polymers such as poly (lactic acid) -PLA, soy-protein, chitin, and starch-based polymers are being used to reduce the dependence on petroleum based resources. The most used natural antioxidants are a-tocopherol, ascorbic acid, quercetin among others. Most of these APF are produced based on the trial and error or base on previous experience. However, researcher have demonstrated that it is difficult to achieve a suitable release rate for different food systems and degradation reactions. The release rates of the antioxidants added to the films are either too slow or too fast. The interactions between the polymer and antioxidants are a key point to estimate their affinity and the rate and total amount of antioxidants released to the food product from the

APF. Several methods can be used to determine the interaction of chemical compounds with polymers such as a Flory-Huggins approach, quantitative structure property relationship (QSPR) [10, 11], and the Hansen solubility parameters [12]. A fast method to determine the relative affinity between a polymer and an additives is the solubility parameter [13]. The term solubility parameter was first used by Hildebrand and Scott. They correlated solubility with cohesive properties of the solvents [12]. The earlier solubility parameter work has a shortcoming, which is limited to regular solutions and does not consider the association between molecules like polar and hydrogen-bonding interactions. Hansen (1967) proposed an extension of the solubility parameter approach to polar and hydrogen- bonding systems. Thus, the Hansen solubility parameters (HSP, δ_d, δ_p, δ_h) are defined as δ_d representing nonpolar part, δ_p representing polar part and δ_h representing hydrogen bonding part. The basic principle of HSP is "like dissolves like". That means the materials with similar HSP have high affinity for each other. Then, the likeness between a polymer and chemical could be estimated by using their HSP [14]. Therefore, the estimation of compatibility between a polymer and chemicals especially antioxidants can help to save time, efforts and money, which are always expended on a new designed packaging system.

1.2 Motivation

As discussed above, more and more attention is given on developing APF based on biodegradable polymers and natural antioxidants. However, most APF are designed based on trials and errors, and the results showed that appropriate release rate for the new designed APF are hard to achieve. To help address this problem, we are proposed to use the HSP theory to estimate the interaction between natural antioxidant and biodegradable polymers. If the compatibility and the release rate between natural antioxidants and biodegradable polymers and

the surrounding environment can be estimated properly, time, resources and funding can be optimally used.

1.3 Goal and objectives

The overall goal of this thesis is to find a method to estimate the release rate of antioxidant from polymers. In this study, the HSP theory is used to describe the affinity between biodegradable polymer and antioxidants. The following tasks are listed to achieve the goal:

1 Determine the HSP for the selected biodegradable polymers and antioxidants by using the Hoy and Van-krevelen method

2 Determine the HSP for the selected biodegradable polymers by using an experimental technique

3 Identify the APF system based on HSP theory to achieve an optimal release of the antioxidant

4 Conduct migration studies on the final processed APF;

5 Analyze and compare the experimental result with the theoretical HSP estimations

REFERENCES

REFERENCES

1. Selke, S.E., J.D. Culter, and R.J. Hernandez, *Plastics packaging: Properties, processing, applications, and regulations*. 2004: Hanser Munich.

2. Decker, E., R. Elias, and D.J. McClements, *Oxidation in Foods and Beverages and Antioxidant Applications: Understanding mechanisms of oxidation and antioxidant activity*. Vol. 1. 2010: Elsevier.

3. Marsh, K. and B. Bugusu, *Food packaging—roles, materials, and environmental issues.* Journal of food science, 2007. **72**(3): p. R39-R55.

4. Choe, E. and D.B. Min, *Mechanisms of antioxidants in the oxidation of foods.* Comprehensive Reviews in Food Science and Food Safety, 2009. **8**(4): p. 345-358.

5. Wanasundara, P. and F. Shahidi, *Antioxidants: Science, technology, and applications.* Bailey's Industrial Oil and Fat Products, 2005.

6. Ashby, R., *Food packaging migration and legislation.* 1997.

7. Miltz, J., et al., *Loss of antioxidants from high-density polyethylene.* Food and Packaging Interactions, ed. by Hotchkiss JH. American Chemical Society, 1988: p. 83-93.

8. Sharma, G., C. Madhura, and S. Arya, *Interaction of plastic films with foods. II, Effect of polyethylene and polypropylene films on the stability of vegetable oils.* Journal of food science and technology, 1990. **27**(6): p. 328-331.

9. Van Aardt, M., et al. *Controlled release of antioxidants from polymeric films to control lipid oxidation in milk.* in *International Animal Agriculture and Food Science Conference, Indianapolis*. 2001.

10. Tehrany, E.A., F. Fournier, and S. Desobry, *Simple method to calculate partition coefficient of migrant in food simulant/polymer system.* Journal of food engineering, 2006. **77**(1): p. 135-139.

11. Luan, F., et al., *QSPR study of permeability coefficients through low-density polyethylene based on radial basis function neural networks and the heuristic method.* Computational materials science, 2006. **37**(4): p. 454-461.

12. Hansen, C.M., *Hansen solubility parameters: a user's handbook*. 2007: CRC.

13. Auras, R., B. Harte, and S. Selke, *Sorption of ethyl acetate and d-limonene in poly (lactide) polymers.* Journal of the Science of Food and Agriculture, 2005. **86**(4): p. 648-656.

14. Hansen, C.M., *Polymer additives and solubility parameters.* Progress in organic coatings, 2004. **51**(2): p. 109-112.

CHAPTER 2 LITERATURE REVIEW

Introduction

This chapter provides a brief introduction of food packaging, including the function of packaging, and the methods used to protect food in food packaging. Then, a section about the main antioxidants (AOx) used in packaging and food is presented. After that the main antioxidant used in plastics and their Hansen solubility parameters (HSP) used to estimate the affinity between polymer and additives are discussed. Finally, the method to test for migration from plastics and the main instruments used to conduct this determination are described.

2.1 A brief introduction of food packaging

Packaging is a very important process to maintain the quality of products during storage, transportation and end-use. The basic functions of packaging are containment, protection, information and convenience [1]. Among them, the main function of food packaging is to achieve preservation and the safe delivery of food products. So, food packaging can contribute to extend the shelf life and maintain the quality and safety of food products. Many packaging materials are used for food packaging, such as metal, glass, paper and plastics. Compare to other materials, plastics have a number of advantages, such as, low cost, light weight, easy to shape, and tailored barrier properties [2]. Food packaging functions have evolved from simple delivers and preservation methods to packaging systems that enhance convenience, safety as well as reducing the environmental impact of the entire product package system [3]. In the last decades, food technologists have focused on how to increase food safety and security [4]. To achieve that, food packaging must actively protect the food product by enhancing their shelf life, which can be fulfilled by adding active or selective barrier properties to the packaging structure. In the food packaging industry, several functional packaging systems including active packaging, modified

atmosphere packaging (MAP) and edible films and coating have been developed to maintain and enhance the quality and shelf-life of food products [4].

Many applications of active packaging have been investigated and created to enhance the safety and security of food products [5]. Active packaging is designed to extend the shelf life of food products, prevents the deterioration of quality and inhibits microbial growth, thus ensuring food safety and quality. Examples of active packaging include oxygen scavenger, moisture absorbers, flavor releasing/absorbing systems, and antioxidants releasing systems.

For oxygen sensitive foods, reducing their exposure to oxygen in the packaging system is very important to keep the shelf life of the product. One method currently uses to delay oxygen uptake or retard food oxidation and rancidity is active packaging. There are different active packaging methods. The inclusion of oxygen scavengers in the form of sachets within the cavity or interior of a package is extensively observed in the market, due to its lower cost and adaptability to different system. However, disadvantage of sachets are the additional packaging operations needed to put a sachet into a package, which increases packaging operations and costs, the need for a particular atmospheric conditions to achieve a targeted scavenging rate, and the chances of being accidentally ingested by minors [6]. Also, scavenging sachets are difficult to be used for liquid food, since direct contact of the liquid food with the sachets may cause leakage of the sachet contents. Other means of controlling the oxygen exposure by the food product is the incorporation of scavenging material (*i.e.*, antioxidants) in the packaging itself and control its release. This method can provide a more uniform scavenging effect throughout the package and its shelf life. Because incorporating the oxygen scavenger into the packaging structure is an efficient way to scavenge oxygen, which will permeate from the outside of the package. So, the lowest possible oxygen in the package system can be achieved [7]. Packaging structures

containing AOxs is an alternative method to reduce the oxidation of food. For a good AOx active packaging to work, the appropriate packaging material and AOxs should be selected. There are certain concerns raised about active AOx packaging, such as whether the added materials will affect processing, and the final properties of the active packaging.

2.2 Antioxidant packaging

2.2.1 Antioxidants

Antioxidants are widely used food additives to improve food stability and extend the shelf-life of oxygen-sensitive foods. AOxs, both synthetic and natural, are very important chemical compounds to prevent oxidative degradation and consequently extend the shelf-life of foods. The structures for some commonly used antioxidants are shown in Table 2.1. Synthetic antioxidants such as propyl gallate (PG), octyl gallate (OG), butylhydroxyanisole (BHA), BHT and tert-butyl-hydroquinone (TBHQ) are commercially used following the regulations of the European Union Directives and Regulations, the FDA in USA, and the Food Standards of Australia and New Zealand [8]. The maximum allowances of these AOxs are regulated by these organizations. Among the synthetic AOxs, PG and BHA are powerful antioxidants widely used to stabilize food from oxidation. Among the natural AOxs, α-tocopherols (Vitamin E), and ascorbic acid (Vitamin C) are commonly used. Catechin, epicatechin, and resveratrol among others AOx are newly being considered. α-tocopherol is a lipid-soluble antioxidant and can be found in many foods like vegetable oils [9]. It is one of most effective radical-chain breaker in unsaturated fatty food. α-tocopherol has be recognized as a safe food additive by The Code of Federal Regulations [10]. The incorporation of α-tocopherol with low- and high- density polyethylene (LDPE and HDPE) has shown to inhibit oxidation of food oxygen sensitive product [11, 12]. Catechin and epicatechin belong to the flavonoid group of AOx and can be found in green tea or in fruits like

grapes [13]. Resveratrol is a phenolic compound of the stibene family, with similar structure to catechin and epicatechin. Resveratrol is commonly found in wines and in various parts of grapes including the skin and the seeds [14]. Radical-scavenging capacity of propyl gallate, ascorbic acid and alpha-tocopherol has been reported lower than resveratrol [15]. Due to consumer demands and market trends, natural AOxs are promising AOxs to be incorporated in polymer films to exert antioxidants effects.

Table 2.1 Structure of antioxidants

Antioxidants	**IUPAC Nomenclature**	**Structure**
BHT	2,6-ditert-butyl-4-methylphenol	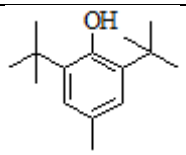
BHA	2-tert-butyl-4-methoxyphenol; 3-tert-butyl-4-methoxyphenol	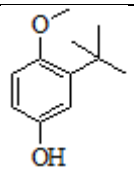
TBHQ	2-tert-butylbenzene-1,4-diol	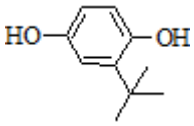
Propyl gallate	propyl 3,4,5 -trihydroxybenzoate	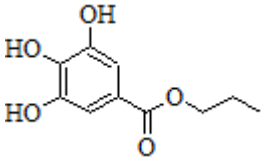
Octyl gallate	Octyl 3,4,5-trihydroxybenzoate	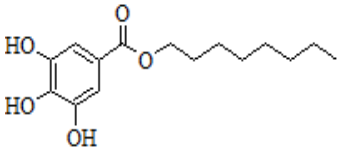
Dodecyl gallate	dodecyl 3,4,5-trihydroxybenzoate	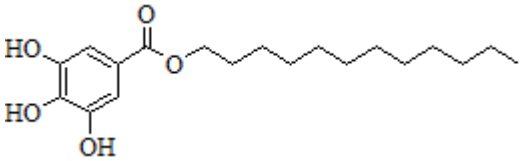

Table 2.1 (cont'd)

Antioxidants	IUPAC Nomenclature	Structure
Ascorbic acid	(5R)-[(1S)-1,2-dihydroxyethyl]-3,4-dihydroxyfuran-2(5H)-one	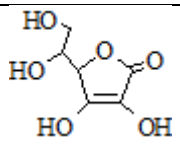
Irganox 1076	octadecyl-3-(3,5-ditert-butyl-4-hydroxyphenyl) propanoate	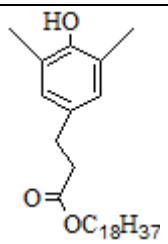
Catechin	(2R,3S)-2-(3,4-dihydroxyphenyl)-3,4-dihydro-2H-chromene-3,5,7-triol	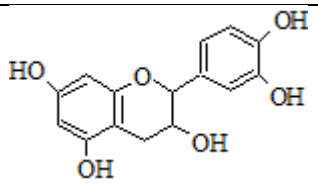
Epicatechin gallate	[(2S-3S)-2-(3,4-dihydroxyphenyl)-5,7-dihydroxy-3,4-dihydro-2H-chromen-3-yl]3,4,5-trihydroxybenzoate	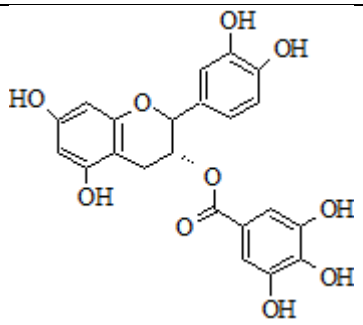
Alpha-tocopherol	5,7,8-trimethyltocol	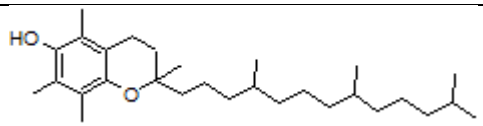
Resveratrol	5-[(E)-2-(4-hydroxyphenyl)ethenyl]benzene-1,3-diol	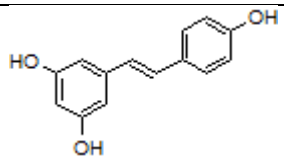

2.2.2 Plastics added with antioxidants

Plastics were introduced as main materials at the beginning of 20th century. Properties such as softness, transparency and low cost, have made plastics essential materials in many industries. Most commercial plastics are petroleum-based synthetic polymers, such as low density LDPE,

polystyrene (PS) and poly (ethylene terephthalate) - PET. Since they are resistant against microbial attack, it cannot be degraded when they are discarded into the environment [16]. With the increasing concerns on environment issues, polymers derived from bio-based resources, which are recyclable and biodegradable have been developed with the intention to reduce the environment pollution caused by plastics. Furthermore, food package are usually contaminated with food, so they cannot practically be recycled. Bio-based and compostable plastics made from renewable resources such as poly (lactic acid) (PLA), poly (hydroxyl-alkanoates) (PHAs), poly (3-hydroxybutyrate) (PHBs) and thermoplastics starch have been developed to try to deal with these issues. These polymers are biodegradable and compostable. Biodegradability depends on the polymer structure, and it is not related to the origin of the material [17]. So, biodegraded polymer can be produced from non-renewable and renewable sources, and it can be defined as biodegradable if they can be mineralized by a natural process.

However, there are still drawbacks with these newly developed polymers. For example, PLA is brittle and have low barrier properties, limiting its application to some extent. As for starch-based materials, they are often very sensitive to moisture conditions, so they mechanical properties are dramatically reduced in humid environment. Another disadvantage of bio-based materials is that they still relatively more expensive than their counterpart petroleum-based polymers.

Polymers unlike glass interact with small molecules, which can be sorb, diffused and desorbed across their structure. AOx polymer uses this principle to release AOx from the polymers and to protect oxygen sensitive food products. AOx packaging is one type of active packaging, in which the antioxidants are incorporated into the plastic films to reduce oxidation of the packed food. The incorporated of AOx can serve dual functions: (1) avoid polymer

degradation during processing, and (2) reduce food oxidation. Extensive research has been done into these systems, mostly from polymers made from non-renewable resources. Research done on oatmeal [18] and vegetable oil [19] have demonstrated that impregnated AOx within plastic films-AOx packaging films (APF)- can increase the storage stability of food since they are released from the polymer. In oatmeal cereals packaged in HDPE film with 0.022% (w/w) BHT and 0.32% (w/w) BHT, HDPE films with lower BHT showed higher oxidation after six weeks storage at 39℃. Marcato *et al*. investigated the migration of AOx additives pentaerythrityl tetrakis(3,5-di-tert-butyl-4-hydroxyphenyl) propionate (Irganox 1010) and tris(2,4-di-tert-butylphenyl) phosphite (Irgafos 168) from polyolefin into oily simulants [20]. The studied polyolefin were isotactic polypropylene homopolymer (PP), ethylene-co-propylene random copolymer (RACO), ethylene-propylene heterophasic copolymer and ethylene-propylene amorphous copolymer blend (EP) and HDPE. The result showed the amount of Irganox 1010 transfer from these plastic materials at 25℃ were different, decreasing in the order EP > RACO > PP > HDPE. The same polyolefin ranking was obtained for Irgafos 168. This information can be used for the selection of polyolefin as raw materials for the production of pharmaceutical and cosmetic containers. However, BHT, Irganox 1010 and Irgafos 168 are synthetic AOx, the addition amount of synthetic antioxidant to food packaging is specifically regulated by the FDA due to human health concerns. There is a growing interest in using natural AOxs in food packaging applications. Therefore, research has been studied combination of natural AOx and bio-based material or biodegradable materials. For example, release of α-tocopherol from PLA films delayed the induction of the oxidation of soybean oil when stored with 2.5% (w/w) α-tocopherol PLA film at 20 and 30℃, comparing with that of oil in contact with PLA without APF [10]. A number of natural AOxs have been incorporated into PLA [10, 13, 21, 22]; however,

few research has been conducted into other polymers like poly (butylene adipate-*co*-terephthalate) (PBAT), which is also compostable. PBAT is currently made from non-renewable resources, but in the future it is expected to be produced from renewable resources.

2.2.3 Biodegradable Polymers

Biodegradable polymers can be identified as: (1) polymers directly extracted from biomass like proteins, lipids, etc.; (2) polymers synthesized by a classical polymerization procedure such as aliphatic-aromatic copolymers, aliphatic polyesters, polylactide aliphatic copolymer (CPLA), using renewable bio-based monomers such as poly (lactic acid) and oil-based monomers like polycaprolactones; and (3) polymers produced by microorganisms and bacteria like polyhydroxylalkanoates [23]. Aliphatic polyesters such as poly(hydroxyl alkanoates) –PHA and synthetic polycaprolactone (PCL), have good biodegradable properties. PHA is produced in microorganism cells and PCL is produced from non-renewable resources. The lack of thermal and mechanical properties of PHAs limits their wide application. Aliphatic-aromatic copolyesters are a more promising alternative as conventional plastics. These plastics present good material properties and biodegradability. These copolyesters are produced from the random polymerization of the diester oligomers of adipic acid/butanediol, and terephthalic acid/butanedoil [24][25].

Poly (butylene adipate-*co*-terephthalate) (PBAT) is an aliphatic-aromatic copolyester that is biodegradable and can be degraded within a few weeks with the aid of naturally occurring enzymes [26]. The structure of PBAT consists of butylene adipate (BA) unit and butylene terephthalate (BT) unit, as showed in figure 2.1. The biodegradability and the material properties are relative to the composition of BA and BT. It has been reported that the optimal compromise between biodegradability and physical properties of PBAT copolyesters can be obtained by a

range from about 35 to 55 mol% of terephthalic acid (TA) (with regard to the total amounts of acid components) [27]. So, adjusting the composition of the aromatic fraction can fulfill the desired application of PBAT copolymers. The great advantage of PBAT copolyesters is that can be synthesized from cheap and widely available bulk chemicals by traditional technical process. Research has shown that thermal and mechanical properties, and the rate of biodegradation all depend on ratio of BA/BT. A range of glass transition temperature (T_g) for PBAT copolymers can be estimated from -61 to -23 °C. Melting temperature (T_m) from 80 to 140 °C can be obtained by altering copolymer composition [27]. PBAT is a flexible and tough polymer designed mainly for film extrusion and extrusion coating [28]. Since PBAT has great biodegradability and high toughness, it becomes an excellent candidate for tough biodegradable polymers such as poly(lactic acid) (PLA) and poly(hydroxybutyrate-*co*-hydroxyvalerate) (PHBV)[29].

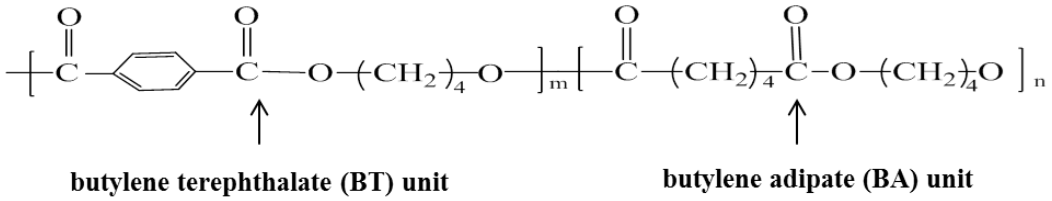

Figure 2.1 Chemical structure of poly (butylene adipate-*co*-terephthalate) (PBAT)

2.3 Interaction between package and food

For oxygen sensitive food, active packaging not only should absorb the excess oxygen but it should also avoid the ingress of oxygen to the package and the release of the oxygen scavenger from the package to protect the food product. In the case of plastic in contact with food, there is always an interaction between the polymer matrix and the food in which small molecules diffuse from one part of the system to another. This interaction is part of the mass transfer occurring within the packaging system. Migration is a mass transfer process, in which low molecular mass

substances initially present in package are released into the contained food, and it is the result of diffusion, dissolution and an equilibrium processes [30]. APF used this mechanism to protect oxygen sensitive food by incorporating AOx in the plastic materials intended to migrate to the food [31]. The AOx transfer through a polymer depends on the interaction between the AOx and the packaging materials as well as the solubility and affinity of the AOx to the food product [32]. If there is a high affinity between the polymer and the AOx, it is hard for the AOx to migrate from the polymer to protect the product. When the likeness between the polymer and the AOx is weak, the AOx migrates to the food too easily, which is also not good for a long extension of the product's shelf life. So, a tailored release is needed to get the right protection. To predict the mass transfer process, it is necessary to estimate the compatibility and affinity between the polymer and the AOx. There is not very much research conducted and reported to estimate the produce compatibility and affinity between the polymer and AOx to design APF.

2.3.1 Solubility parameter

Solubility parameters, in particular the Hansen solubility parameters (HSP), have been shown useful to correlate polymer solution phenomena and chemical resistance since the HSP are easy to calculate or experimentally determined [32]. The initial concepts of the solubility parameter was developed by Scatchard and subsequently greatly extended by Hildebrand [33]. The solubility parameters have been used to select solvents for coatings materials for many years. A series of improvements and other application in solubility parameter has been made over the years, such as to predict compatibility of polymers, chemical resistance, and permeation rates, and characterize the surfaces of pigments or fibers [34].

The total solubility parameter was first introduced by Hildebrand and Scott [34]. The Hildebrand solubility parameter δ_t is defined as the square root of the cohesive energy density (CED):

$$\delta_t = (CED)^{\frac{1}{2}} = (\frac{\Delta E_v}{V})^{1/2} \qquad 2.1$$

$$\Delta E_v = \Delta H_v - RT \qquad 2.2$$

As the equation 2.1 expresses, δ_t is calculated by dividing the energy of vaporization for the pure solvent, ΔE_v, by the molar volume, V, of the involved liquid, and making the square root of this number. The energy of vaporization for the liquid is calculated by equation 2.2, where ΔH_v is the heat of vaporization for the liquid, R is the universal gas constant, and T is the absolute temperature. The common used unit for δ_t in the USA is $(cal/cm^3)^{1/2}$. The SI unit for it is $MPa^{1/2}$, which is 2.0455 times larger than that in the former unit. The basic principle to using the solubility parameter is "like dissolves like". Liquids with similar solubility parameters will be miscible. Also, polymers will dissolve in solvents whose solubility parameters are similar with them. Therefore, the affinity of a polymer and solvent can be predicted by using solubility parameters.

2.3.2 Hansen solubility parameters

A shortcoming of the earlier solubility parameter work is that the approach was limited to regular solutions [35], since other interaction could exist between molecules such as polar and hydrogen-bonding interactions. To attempt to improve on this, several researchers have been working on it. A recolection of the research and advances can be found in Barton's extensive book [36]. The work made by Gardon and Teas is also a good source [37]. The approach of Blanks and Prausnitz divided the solubility parameter into "nonpolar" and "polar" [38]; the approach of Burrell divided solvents into hydrogen bonding classes. Blanks and Prausnitz's

approach greatly influenced Hansen's earlier work [34]. Hansen proposed an extension of the single Hildebrand solubility parameter to three components solubility parameters (nonpolar, polar and hydrogen-bonding parameters), now call the Hansen solubility parameters (HSP). This is based on the fact that all types of physical bonds are broken when they are evaporated including those three kinds of bonds. As mentioned before, materials with similar Hildebrand solubility parameters should have high affinity for each other. However, in some cases, this is not applicable. For example, the Hildebrand solubility parameter of ethylene carbonate and methanol are identical, 29 $MPa^{1/2}$, but their solvencies are different [39]. This can be illustrated by HSP of these two solvent. For ethylene carbonate,δ_d, δ_p and δ_h are 18 $MPa^{1/2}$, 21.7 $MPa^{1/2}$, 5.1 $MPa^{1/2}$ respectively, and for methanol, δ_d, δ_p and δ_h are 15.1 $MPa^{1/2}$, 12.3 $MPa^{1/2}$, 22.3 $MPa^{1/2}$ respectively. It is easily noticed that the HSP of these two solvents are not the same. This phenomenon can never been predicted by the Hildbrand solubility parameters. There are three types of interaction included in HSP concept.

Nonpolar interaction (δ_d) — The most general one is nonpolar interaction, which is derived from atomic forces and also named dispersion interactions in the literature [34]. All molecules contain this type of attractive forces since molecules are built up from atoms.

Polar interaction (δ_p) — Polar interaction are inherently molecular interactions and found in most molecules to one extent or another [34]. It is caused by permanent dipole. The molecular dipoles occur when there is an unequal sharing of electrons between atoms in a molecule. The dipole moment is the primary parameter which is used to calculate polar interactions.

Hydrogen bonding interaction (δ_h) — The basis of the hydrogen bonding interaction is the molecule attraction because of hydrogen bond. This can be called electron exchange

parameter. In HSP approach, the hydrogen bonding parameters are defined to more or less collect the energies from interactions not included in other two parameters [34].

2.3.3 Methods used to measure HSP

According to the HSP concept, the total cohesion energy E must be the sum of three individual energies, as expressed in equation 2.3. Also the relationship of Hildebrand solubility parameters with HSP is found as equation 2.4.

$$E = E_D + E_P + E_H \qquad 2.3$$

$$\delta_t^2 = \delta_d^2 + \delta_p^2 + \delta_h^2 \qquad 2.4$$

Thus, the HSP is considered as a more reliable method to estimate the affinity of a polymer and a solvent.

Theoretical and experimental methods can be used to estimate the HSP of a material. When the experimental data for the test material is not available, the group contribution can be used as a first estimate of the solubility behavior of a material. It is recommended to always confirm the HSP for polymers determined by group contributions with experimentally determined HSP [34].

2.3.4 The experimental method

The experimental method to determine HSP for a polymer is to evaluate whether or not it dissolves in selected solvents. Experimental data is based on the observation of the interaction between studied materials and well-known solvents. A lot of different phenomena will be observed including full solution, degree of swelling by visual observation, clarity, surface attack, etc. The solvents that have similar or close HSP to the studied material will dissolve the material; on the other hand, if any visual change is observed, there is assumed that little interaction between the solvent and studied material exist. These different interactions are used to divide the

solvents into two groups, one which is considered "good" and the other which is considered "bad" [34]. "Good" solvents have strong interaction with the studied material, indicating that they have closer HSP to materials studied than "bad" solvents. Various ways can be used to generate and treat experimental data, like using a score scale to rank the different interactions happening with the selected solvents. This data can then be processed to determine the HSP parameters. The three HSP parameters and the radius value, R_o, of the sphere of interaction for materials can be obtained from these calculations. Mainly, a sphere of interaction is determined for the solvents and the material. R_o is the radius of interaction for the studied material, which gives the maximum difference allowed to define a good interaction between the solvents and materials or other two materials. To evaluate whether or not a material belongs to a sphere of high affinity of another material, the distance R_a between these two materials can be calculated by the equation 2.5. δ_d , δ_p and δ_h refer to the dispersion, polar and hydrogen parameters respectively. The subscripts present the different materials.

$$R_a^2 = 4\,(\delta_{d2} - \delta_{d1})^2 + (\delta_{p2} - \delta_{p1})^2 + (\delta_{h2} - \delta_{h1})^2 \qquad 2.5$$

$$RED = Ra/Ro \qquad 2.6$$

The ratios between *Ra* and *Ro* is called the Relative Energy Difference (*RED*), see the equation 2.6. This parameter can be referred to find whether a material is within the sphere of affinity of other studied material or solvents. Good interactions of materials always show a *RED* number less than 1.0. The RED number 1 means the material is right on the soluble/insoluble border [39]. Fig 2.1 shows a three-dimensional graph of equations 2.5 and 2.6. It is easy to visualize the solubility properties, and the distance between materials. The HSP coordinates of a material are located in the center of sphere with radius R_o. R_a is the distance between the studied material and specified solvent or material.

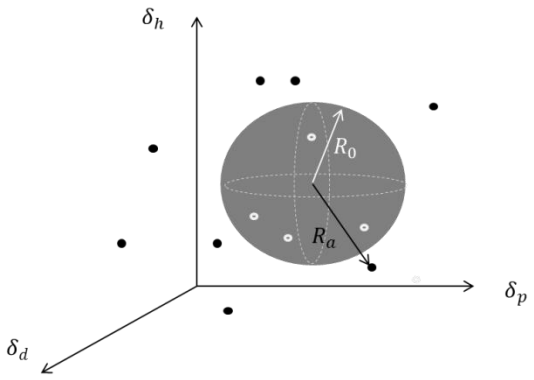

Figure 2.2 HSP sphere with dots representing the selected solvents or materials, modified from Jing Ma' *et al*.[40]

2.3.5 Group contributions calculation

There are a limited number of solvents and material, which HSP values have been already determined. Measuring the HSP through experimental method is time consuming. Therefore, methods to predict the HSP are highly valuable. One of the useful prediction method is based on the molecular structure of a material. However, the available experimental data indicates that it is impossible to use a calculation methods from the chemical structure for an accurate prediction of solubility parameter components [41]. However, such prediction method can provide a rough estimation of HSP, which is useful when there is no available data. There are two highly published methods, Hoftyzer and Van Krevelen (1976) and Hoy (1985). Both methods have the same basic assumption, as expressed in equations 2.3 and 2.4. Van Krevelen and Hoy both proposed a set of group contribution values of cohesive energy *E*, and the molar attraction constant *F* which is related with the cohesive energy *E* [41]. Van Krevelen (1965) derived a set of atomic contributions to calculate *F*, which derive in an indirect way to the values of *E* for polymers. The structure of studied materials can be broken down into several different groups, which have their own *F* and *E* values referred from the group contribution values. Values for *F* can be obtained by the published tables depending on the used method [41]. Based on *F*

and *E* values of the group contribution method, the HSP of a material could be estimated by the equations by either the Hoftyzer-Van Krevelen or Hoy methods. The usages of both methods are easily implemented.

2.4 Migration process

Due to the increasing concerns about health matters among consumers, the importance of migration of substances from food packaging to food has attracted increasingly attention.

Migration can be considered as the desorption process of chemical compounds from the packaging material into the product. The interaction of packaging materials with the food can strongly affect the migration process. The released components called migrants such as monomers and additives are common migrants in packaging materials. Migrants can be sensitive to human health, so they are regulated by the EU (European Union) and the FDA (Food and Drugs Administration). Legally, polymers for packaging are regulated through global or specific migration levels [42]. Global migration measures the total amount of compounds migrated to a food simulant under the designed temperature and time conditions. However specific migration is to measure the migration of a specific chemical component. Due to the toxicity of a specific component, it is important to conduct specific migration.

The migration process in packaging systems specially in polymers is influenced by the diffusion and partition coefficients [43]. The diffusion coefficient (D) provides information on the migration rate, and it is affected by the molecular structure, weight, and affinity of the migrant to the food simulant and/or food, and the affinity of the polymer to the migrant [44]. The partition coefficient ($K_{p/s}$) provides information on the quantity transferred from a polymer to a food at equilibrium, and it is affected by the solubility and affinity between the polymer phase and food product phase. The diffusion process in migration is mostly described by Fick's laws of

diffusion [45]. The Fick first law of diffusion at steady state for one dimension of a migrant from a polymer is expressed by equation 2.7. For unsteady state in one dimension, the Fick second law is used, as expressed in equation 2.8.

$$F = -D_p \frac{\partial C_p}{\partial X} \qquad 2.7$$

$$\frac{\partial C_P}{\partial t} = D_P \frac{\partial^2 C_P}{\partial X^2} \qquad 2.8$$

where F is the transfer rate of the migrant per unit area, D_P is the diffusion coefficient of the substance in the polymer (cm^2/s), C_P is the migrant concentration in the polymer (g migrants/g polymer), X is the diffusion distance (cm), and t is the elapsed time (s).

2.4.1 Effect of temperature on diffusion

During the diffusion process, the effect of temperature is an important factor, which affects the mobility of migrants in polymeric materials and influences the diffusion process. When temperature is higher than the T_g of the polymer, the polymer is at the rubbery state, which enhances the diffusion process. When the temperature is lower than T_g of the polymer, the polymer is at glass state. Due to the restriction of the polymer chains, it requires more time for the migrants to be transported through the polymer matrix and to reach an equilibrium state.

2.4.2 Diffusion models for migration process

Migration processes are described by the diffusion kinetics of migrant in the film and it is expressed by the diffusion coefficient (D). According to the Fick's second law, different solution of a system can be obtained depending on the boundary conditions of the system that we are solving for as expressed by equations 2.9 and 2.12 for one-dimension diffusion[44]. A the initial time (t=0), there is no migration happening between the package and the food, so the migrant concentration in the food is zero. When the migration begins to occur in the film and the food

system, the amount of migrant, which is migrated from the film, will be equal to the amount existing in the food during the migration process. When the diffusion is in one-dimension and in a limited volume of film in finite volume of solution, equation 2.9 is used.

$$\frac{M_t}{M_\infty} = 1 - \sum_{n=1}^{\infty} \frac{2\alpha(1+\alpha)}{1+\alpha+\alpha^2 q_n^2} \exp\left(-\frac{D q_n^2 t}{l^2}\right) \qquad 2.9$$

where M_t/M_∞ is the concentration of the antioxidant diffused at time *t* divided by the concentration of the antioxidant diffused at equilibrium; *l* is the thickness of the film and the q_n are the non-zero positive roots of tan $q_n = \alpha q_n$ and α as expressed by equation 2.10:

$$\alpha = \frac{V_S}{V_P \cdot K_{P,S}} \qquad 2.10$$

where V_S and V_P are the volume of the simulant and the polymer. $K_{P,S}$ is the partition coefficient of antioxidant between the polymer and the simulant, which can be assumed constant at a lower concentration and calculated from the ratio of the concentration of the antioxidant in the film ($C_{P,\infty}$, µg/cm^3) and the simulant ($C_{S,\infty}$, µg/cm^3) at equilibrium according to following equation:

$$K_{P,S} = \frac{C_{P,\infty}}{C_{S,\infty}} \qquad 2.11$$

When the diffusion happens in one-dimension and in a limited volume of film in infinite volume of solution, equation 2.12 is applied,

$$\frac{M_t}{M_\infty} = 1 - \frac{8}{\pi^2} \sum_{m=1}^{\infty} \frac{1}{(2m+1)^2} \exp\left(-\frac{D(2m+1)^2 \pi^2 t}{l^2}\right) \qquad 2.12$$

Equation 2.12 is a simplified solution, which is used for the case that the amount of simulant can be considered infinite (i.e., $\alpha \gg 1$ since $V_S \gg V_P$ and /or $K_{P,S} < 1$).

2.5 Methods for measuring migration

Migration testing is mostly carried out according to specific regulation. In the US, the FDA is the governing body providing regulations and methods for migration testing. The FDA also provides the guidance and recommendations for industry to perform migration studies. Migration testing is controlled by appropriate laboratory conditions. The main intention in a migration experiment is always to simulate the migration process as happened in a real case. The purpose of rules and legislations related to migration is to assure the safety of the materials used in contact with food and to guarantee consumer's safety.

2.5.1 Migration cell

The migration cells to run migration experiments are normally made of a glass container or unreactive plastic in general of amber color to avoid photo degradation. According to the FDA guidance, for a general migration study a specimen of known surface area and a known volume of food simulant are used in the migration cell [46]. The two-sided migration cell is recommended as shown in Figure 2.3. Although this specific cell may not be universally applicable, the modified design with two essential features are recommended by FDA: (1) inert spacers (such as glass beads) are used to separate polymer films or sheets to allow the food simulant flows freely around each film or sheet; (2) a gas-tight and liquid-tight seals are maintained where the headspace is minimized. For some application, such as lamination structure, two-sided migration cell would be replaced by other cell designs as explained by the FDA.

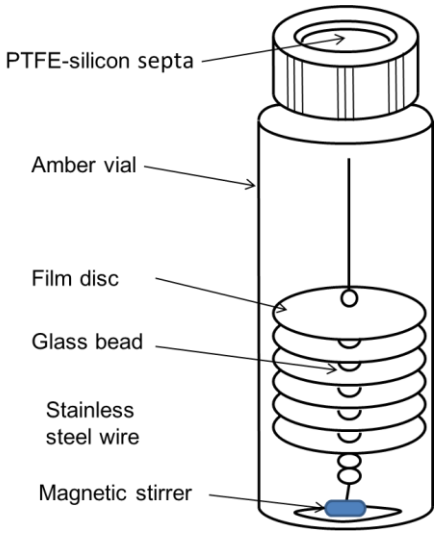

Figure 2.3 Migration cell

2.5.2 Food simulant selection

Migration testing is usually performed using food simulant to mimic real food and to facilitate detection of the migrant chemical compound. The food simulants recommended by the FDA are listed in table 2.2.

Table 2.2 Food simulants recommended by the FDA

Food-type	Recommended Simulant
Aqueous & Acidic foods	10% ethanol
Low- and High-alcoholic foods	10% or 50% ethanol
Fatty foods	Food oil (e.g corn oil), HB307, Miglyol 812, or others

The information about migration cells provided by the FDA serves as recommendation. Actually, there are many other testing methods provided by organizations such as the European Commission, MERCOSUR and Japan legislations. For unsaturated food oil (like olive oil, corn oil), since they are susceptible to oxidation, especially at high temperature, it is difficult to test them. So, HB307 and Miglyol 812 could be acceptable as a fatty-food simulant since they are composed of saturated carbons. The FDA provides a list of various polymers and their

recommended fatty-food stimulants to effectively help to simulate food oil [46]. The volume of simulant to specimen surface area ratio should reflect properly the value in actual food packaging, so a ratio between 155 and 0.31mL/cm^2 is generally recommended.

2.5.3 Temperature and time selection for migration testing

Migration protocols recommended by the FDA use short-term accelerated testing to simulate migration in real situation. For room temperature applications, a test with temperature 40 ℃ (104 ℉) for 10 days is recommended. This test method can approximately reflect the equivalent levels of migration obtained from extended storage (6 -12 months) at 20 ℃ (68℉). For frozen or refrigerated food application, the test temperature recommended is 20 ℃ (68 ℉). Other temperature and exposure time could be recommended depending on different situations. For each migration experiment, the FDA recommends that at least for four time intervals the test solutions should be analyzed. For example, for the 10 days (240 hours) exposure, the recommended sampling times are 2, 24, 96 and 240 hours. Also the analysis of a blank or control is recommended to use.

2.6 Liquid chromatography for characterization and analysis

Liquid chromatography (LC), especially high-performance liquid chromatography (HPLC) is commonly applied to identify and quantify specific migrants in migration studies. Sample preparation is the first step for an HPLC analysis. Solvent extraction is a commonly used technique for antioxidant extraction from polymers. The chemical compounds from a polymeric film are extracted in a solvent at specific temperature and for a certain time. The extracts can then be injected into an HPLC system directly for the quantification analysis. The separation of the studied antioxidant from other chemical compounds in the extract is carried out in the column which is installed into the HPLC equipment and designed to identify these compounds.

Different type of columns are used as stationary phase and different mix of solvents are used as carried or mobile phases [47]. The elution of the mobile phase in the HPLC system can be either isocratic or gradient depending on the composition of the sample and the detector used in the HPLC system. Various detectors are used for an HPLC, such as ultra violet (UV) detector, fluorescence (FL) detection and mass spectrometry (MS) detection. UV absorption detector can analyze the chemical compounds based on their varying degrees of absorption in the UV regions. Compounds with aromatic rings, C=C double bonds or some other functional groups, they all have a specific positive absorption of UV light at certain wavelength. These wavelengths are easily measured by UV-HPLC. As for fluorescence detector in HPLC, molecules are excited with intense UV emission lines from a mercury lamp or wavelengths isolated by filters from a xenon lamp [47]. This permits an optimal sensitivity for a wide range of analytes. Even though fluorescence detector can provide several orders of magnitude greater sensitivity for those compounds which do display fluorescence emission compared with UV absorption detector, there is only limited subset of analytes that can display fluorescence emission. MS detection is carried out by using electrospray ionization (ESI) and atmospheric pressure chemical ionization (APCI), and it provides more reliable identification compared to UV and fluorescence detectors.

REFERENCES

REFERENCES

1. Barlow, S., *The role of the Scientific Committee for Food in evaluating plastics for packaging.* Food Additives & Contaminants, 1994. **11**(2): p. 249-259.

2. Coles, R., D. McDowell, and M.J. Kirwan, *Food packaging technology*. 2003: Blackwell Oxford.

3. Stilwell, E.J., *Packaging for the environment: a partnership for progress.* 1991.

4. Han, J.H., *New technologies in food packaging: overview.* Innovations in food packaging, 2005. **1**.

5. Rooney, M.L., *Overview of active food packaging*. 1995: Springer.

6. elangovan, D., *Charaterization of metal organic framework and polymer composites and the method of their preparation*, in *School of package*. 2010, Michigan state univeristy: east lansing.

7. Ching, T.Y., *Oxygen scavenging ribbons and articles employing the same*. 1998, Google Patents.

8. André, C., et al., *Analytical strategies to evaluate antioxidants in food: a review.* Trends in Food Science & Technology, 2010. **21**(5): p. 229-246.

9. Min, D. and J. Boff, *Chemistry and reaction of singlet oxygen in foods.* Comprehensive Reviews in Food Science and Food Safety, 2002. **1**(2): p. 58-72.

10. Manzanarez-López, F., et al., *Release of α-Tocopherol from Poly (lactic acid) films, and its effect on the oxidative stability of soybean oil.* Journal of Food Engineering, 2011. **104**(4): p. 508-517.

11. Mallégol, J., D. Carlsson, and L. Deschenes, *Antioxidant effectiveness of vitamin E in HDPE and tetradecane at 32 C.* Polymer Degradation and Stability, 2001. **73**(2): p. 269-280.

12. Al-Malaika, S., H. Ashley, and S. Issenhuth, *The antioxidant role of α-tocopherol in polymers. I. The nature of transformation products of α-tocopherol formed during melt processing of LDPE.* Journal of Polymer Science Part A: Polymer Chemistry, 1994. **32**(16): p. 3099-3113.

13. Iñiguez-Franco, F., et al., *Antioxidant Activity and Diffusion of Catechin and Epicatechin from Antioxidant Active Films Made of Poly (l-lactic acid).* Journal of agricultural and food chemistry, 2012. **60**(26): p. 6515-6523.

14. Soleas, G., et al., *A derivatized gas chromatographic-mass spectrometric method for the analysis of both isomers of resveratrol in juice and wine.* American journal of enology and viticulture, 1995. **46**(3): p. 346-352.

15. Soares, D.G., A.C. Andreazza, and M. Salvador, *Sequestering ability of butylated hydroxytoluene, propyl gallate, resveratrol, and vitamins C and E against ABTS, DPPH, and hydroxyl free radicals in chemical and biological systems.* Journal of agricultural and food chemistry, 2003. **51**(4): p. 1077-1080.

16. Madhavan Nampoothiri, K., N.R. Nair, and R.P. John, *An overview of the recent developments in polylactide (PLA) research.* Bioresource Technology, 2010. **101**(22): p. 8493-8501.

17. Witt, U., et al., *Biodegradable polymeric materials—not the origin but the chemical structure determines biodegradability.* Angewandte Chemie International Edition, 1999. **38**(10): p. 1438-1442.

18. Miltz, J., et al., *Loss of antioxidants from high-density polyethylene.* Food and Packaging Interactions, ed. by Hotchkiss JH. American Chemical Society, 1988: p. 83-93.

19. Sharma, G., C. Madhura, and S. Arya, *Interaction of plastic films with foods. II, Effect of polyethylene and polypropylene films on the stability of vegetable oils.* Journal of food science and technology, 1990. **27**(6): p. 328-331.

20. Marcato, B., et al., *Migration of antioxidant additives from various polyolefinic plastics into oleaginous vehicles.* International journal of pharmaceutics, 2003. **257**(1): p. 217-225.

21. Ortiz-Vazquez, H., et al., *Release of butylated hydroxytoluene (BHT) from Poly (lactic acid) films.* Polymer Testing, 2011. **30**(5): p. 463-471.

22. Soto-Valdez, H., R. Auras, and E. Peralta, *Fabrication of poly (lactic acid) films with resveratrol and the diffusion of resveratrol into ethanol.* Journal of Applied Polymer Science, 2011. **121**(2): p. 970-978.

23. Siracusa, V., et al., *Biodegradable polymers for food packaging: a review.* Trends in Food Science & Technology, 2008. **19**(12): p. 634-643.

24. Javadi, A., et al., *Processing and characterization of solid and microcellular PHBV/PBAT blend and its RWF/nanoclay composites.* Composites Part A: Applied Science and Manufacturing, 2010. **41**(8): p. 982-990.

25. Herrera, R., et al., *Characterization and degradation behavior of poly (butylene adipate-co-terephthalate) s.* Journal of Polymer Science Part A: Polymer Chemistry, 2002. **40**(23): p. 4141-4157.

26. Witt, U., et al., *Biodegradation of aliphatic–aromatic copolyesters: evaluation of the final biodegradability and ecotoxicological impact of degradation intermediates.* Chemosphere, 2001. **44**(2): p. 289-299.

27. Witt, U., R.-J. Müller, and W.-D. Deckwer, *Biodegradation behavior and material properties of aliphatic/aromatic polyesters of commercial importance.* Journal of environmental polymer degradation, 1997. **5**(2): p. 81-89.

28. Gu, S.-Y., et al., *Melt rheology of polylactide/poly (butylene adipate-< i> co</i>-terephthalate) blends.* Carbohydrate Polymers, 2008. **74**(1): p. 79-85.

29. Javadi, A., et al., *Processing and characterization of microcellular PHBV/PBAT blends.* Polymer Engineering & Science, 2010. **50**(7): p. 1440-1448.

30. rubino, M., *Permeability ans shelf life*, S.o. package, Editor. 2012: east lansing.

31. Contini, C., et al., *Development of active packaging containing natural antioxidants.* Procedia Food Science, 2011. **1**: p. 224-228.

32. Auras, R., B. Harte, and S. Selke, *Sorption of ethyl acetate and d-limonene in poly (lactide) polymers.* Journal of the Science of Food and Agriculture, 2005. **86**(4): p. 648-656.

33. Hildebrand, J. and R. Scott, *The Solubility of Nonelectrolytes, Reinhold Publ.* Corp, New York, 1950.

34. Hansen, C.M., *Hansen solubility parameters: a user's handbook*. 2007: CRC.

35. Hildebrand, J.H. and R.L. Scott, *Regular solutions*. 1962: Prentice-Hall Englewood Cliffs, NJ.

36. Barton, A., *Handbook of Solubility Parameters and other Cohesion ParametersCRC*. Baton Rouge, FL, 1983: p. 82.

37. Myers, R.R. and J.S. Long, *Characterization of coatings: physical techniques*. Vol. 2. 1976: Dekker.

38. Blanks, R.F. and J. Prausnitz, *Thermodynamics of polymer solubility in polar and nonpolar systems.* Industrial & Engineering Chemistry Fundamentals, 1964. **3**(1): p. 1-8.

39. Auras, R.A., et al., *Poly (lactic acid): synthesis, structures, properties, processing, and applications*. Vol. 10. 2011: Wiley.

40. Ma, J. and R.M. Larsen, *A COMPARATIVE STUDY ON DISPERSION AND INTERFACIAL PROPERTIES OF SWNTS/POLYMER COMPOSITES USING HANSEN SOLUBILITY PARAMETERS.* ACS applied materials & interfaces, 2013.

41. Van Krevelen, D.W. and K. Te Nijenhuis, *Properties of polymers: their correlation with chemical structure; their numerical estimation and prediction from additive group contributions*. 2009: Elsevier Science.

42. Garde, J.A., R. Catalá, and R. Gavara, *Global and specific migration of antioxidants from polypropylene films into food simulants.* Journal of Food Protection®, 1998. **61**(8): p. 1000-1006.

43. Koszinowski, J. and O. Piringer, *Food/package compatibility and migration.* Journal of Plastic Film and Sheeting, 1987. **3**(2): p. 96-111.

44. Crank, J., *The mathematics of diffusion*. 1979: Oxford university press.

45. Hernandez, R. and J. Giacin, *Factors affecting permeation, sorption and migration processes in package-product systems.* Food storage stability, 1998: p. 269-330.

46. FDA, U., *CFSAN. Guidance for Industry-Preparation of Premarket Notifications for Food Contact Substances: Chemistry Recommendations*.

47. Robinson, J.W., E.M.S. Frame, and G.M. Frame II, *Undergraduate instrumental analysis*. 2004: CRC Press.

CHAPTER 3 MATERIALS AND METHODS

3.1 Materials

Alpha-tocopherol (α-TOC) (95% HPLC), propyl gallate (PG) (≥98% HPLC), butylated hydroxytoluene (BHT) (≥99% HPLC), ethanol (200 proof HPLC), and methanol (≥99.9% HPLC) were all purchased from Sigma-Aldrich, St. Louis, MO, USA. Water (HPLC grade) was obtained from J.T.Baker, Center Valley, PA, USA. Poly (butylene adipate-*co*-terephthalate) (PBAT) resin with a density of 1.25-1.27 g/cc (Ecoflex F Blend C1200) was obtained from BASF chemical company (TX, USA). Migration cell of 40 mL amber vials with slide valve caps with PTFE-silicon septa was procured from Sigma-Aldrich, St. Louis, MO, USA. Stainless steel wire, glass beads, and magnetic stirrer were obtained from VWR, Radnor, PA, USA.

3.2 Methods

3.2.1 Hansen solubility parameters (HSP)

In order to determine the HSP an experimental method and theoretical group contribution methods were used.

3.2.1.1 Experimental method for determining HSP

Table 3.1 shows the HSP parameters of the 17 solvents used to determine the HSP of PBAT. Equal amounts (2 g) of PBAT were dissolved in 10 ml of solvent for each vial. Vials with PBAT were sonicated for 15 min before visual observation.

Table 3.1 Solvents used for determining the Hansen's solubility parameters

Solvent Number	**Solvent**	**δ_d(mJ/m^2)**	**δ_p (mJ/m^2)**	**δ_h (mJ/m^2)**
1	Dichloromethane	18.2	6.3	6.1
2	Toluene	18	1.4	2
3	Tetrachloroethane	18.8	5.1	5.3
4	Methyl Ethyl Ketone	16	9	5.1
5	Cyclohexane	16.8	0	0.2
6	Diethylene Glycol	16.6	12	20.7
7	Chloroform	17.8	3.1	5.7
8	Acetone	15.5	10.4	7
9	THF	16.8	5.7	8
10	Acetonitrile	15.3	18	6.1
11	Dimethyl Sulfoxide	18.4	16.4	10.2
12	Ethyl Acetate	15.8	5.3	7.2
13	Methanol	15.1	12.3	22.3
14	Phenol	18	5.9	14.9
15	DMF	17.4	16.7	11.3
16	Hexane	14.9	0	0
17	Ethanol	15.8	8.8	19.4

The basic principle of HSP is that "like dissolves like", which means materials with similar HSP have high affinity for each other. In the three dimensional Hansen space, three parameters can be treated as coordinates to help estimate the affinity between materials. Based on the basic principle of HSP, the nearer two materials positioned in Hansen space, the more likely they are to dissolve into each other. The interaction radius (R_o) is introduced to determine if the parameters of materials (the antioxidant, polymer and food simulant in this study) are within in range of solubility. This value is the radius of sphere in the Hansen space and the center of this sphere is determined by HSP. The distance between different HSP in the Hansen space was calculated by equation 3.1:

$$R_a^2 = 4\,(\delta_{d2} - \delta_{d1})^2 + (\delta_{p2} - \delta_{p1})^2 + (\delta_{h2} - \delta_{h1})^2 \qquad 3.1$$

The subscripts 1 and 2 in the equation represent the dispersive, polar and hydrogen bond energy of the two studied materials, respectively.

After calculation of the distance between chemical and/or materials, the relative energy difference (*RED*) is also recommended to use, which is easy for the visual estimation. *RED* is given by following equation:

$$RED = R_a / R_o \qquad 3.2$$

The general guideline:

RED< 1: the molecules are alike and will dissolve each other

RED= 1: the system is right on the soluble/insoluble border

RED> 1: the system will not dissolve

In order to obtain the sphere of solubility, the mix of the 17 solvents used to solve PBAT were labeled in an arbitrary scale between 1 and 6 based on the degree of solubility of PBAT in the solvent as shown in Table 3.2.

Table 3.2 Scoring scale for determining the Hansen solubility parameters

Score	**comments**
1	Easy to be dissolved
2	Take a bit of efforts to be dissolved completely
3	Take a bit of efforts to be dissolved most
4	Swell a lot, and gel
5	Swell a little, settle down at bottom
6	No change, just settle down

3.2.1.2 Hoftyzer and Van-Krevelen theoretical estimation method of HSP

The Hoftyzer and Van-Krevelen method can be used to predict the three solubility parameter components through the group contribution approach. Equations 3.3 to 3.5 were used to determine them:

$$\delta_d = \frac{\sum F_{di}}{V} \qquad 3.3$$

$$\delta_p = \frac{\sqrt{\sum F_{pi}^2}}{V} \quad 3.4$$

$$\delta_h = \sqrt{\frac{\sum E_{hi}}{V}} \quad 3.5$$

where,

F_{di} is the group contributions to dispersion component of molar attraction constant, J $^{1/2}$.cm $^{3/2}$/mol

F_{pi} is the group contributions to polar component of molar attraction constant, J $^{1/2}$.cm $^{3/2}$/mol

E_{hi} is the group contributions to hydrogen bonding energy component, J/mol

V is molar volume of calculated material, cm^3/mol

Analysis of HSP parameters —The experiment method and the Hoftyzer and Van-Krevelen method were conducted to get the HSP values of PBAT. All the HSP values for the antioxidants, polymers and solvents were obtained through the Hoftyzer and Van-Krevelen method. Selected compounds were also obtained from literature. Base on the basic principle of HSP- "like dissolves like", the distance between the two different materials can estimate the affinity between them. In order to clearly display the distance between them, a 3D plot of three HSP parameters was created. These three parameters can be treated as coordinates of the radius of a sphere in a 3D space. Plots were created by using MATLAB R2011b (MathWorks, Natick, MA, USA).

3.2.2 Production of PBAT- α-tocophorol (PBA) and PBAT-Propyl gallate (PBP) Film

Figure 3.1 shows a sketch of the entire production process of the antioxidant films. In order to obtain 2% w/w PBA films and 2% w/w PBP films and PBAT control (PBC) film, 20% α-TOC of PBAT master batch (PBAM), 20% PG of PBAT master batch (PBPM) and PBAT without antioxidants as a control (PBCM) were first prepared by ZSK 30 Twin-screw extruder (Werner and Pfleiderer, NJ, USA). α-TOC (200 g) was mixed directly with 800 g PBAT resin then

introduced into the hopper. To get 20% PBPM, PBAT resin from a feeder machine Schenck AccuRate (Whitewater, WI, USA) was introduced at 90 g/min and mixed with PG in the hopper which was came from another feeder machine Schenck AccuRate (Whitewater, WI, USA) at 22.2 g/min of feed rate (Figure 3.2). Extrusion temperatures for the master batch from zone 1 through zone 6 of the extruder were 110-125-145-150-160-155℃, respectively. A screw speed of 123 rpm was used. The extruded filament was immediately cooled through a water bath, Then, a pelletizer from Scheer Bay Co. (MI, USA) was used to ground the filaments.

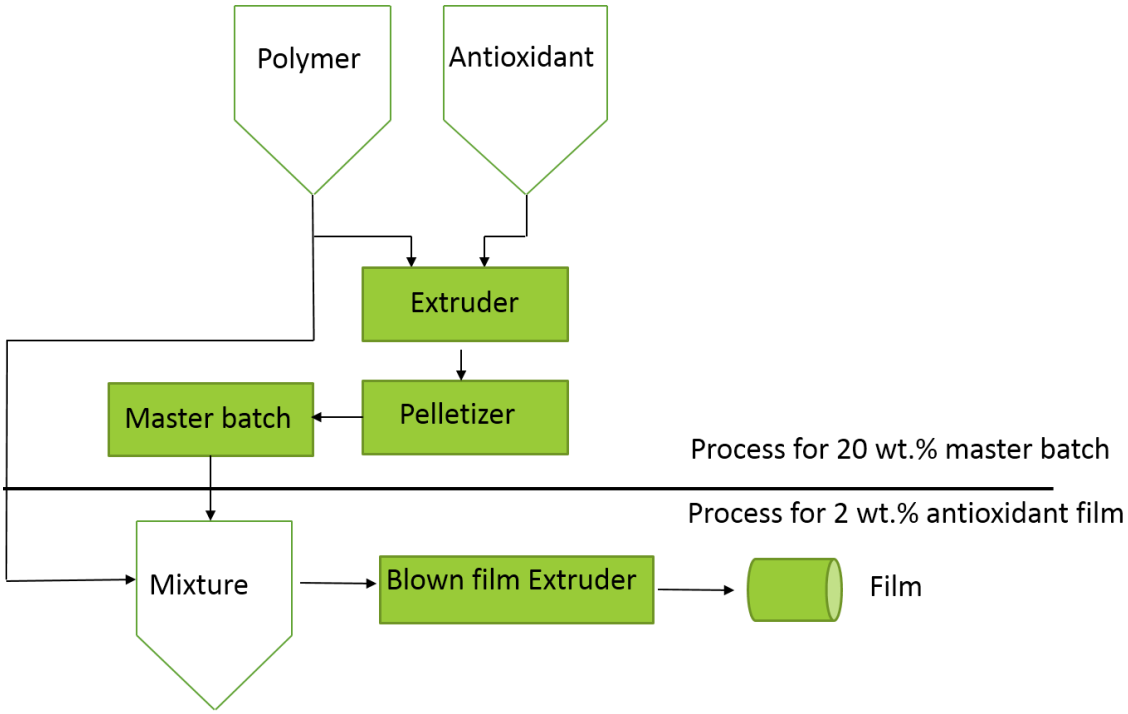

Figure 3.1 Schematic process for the production of antioxidants film

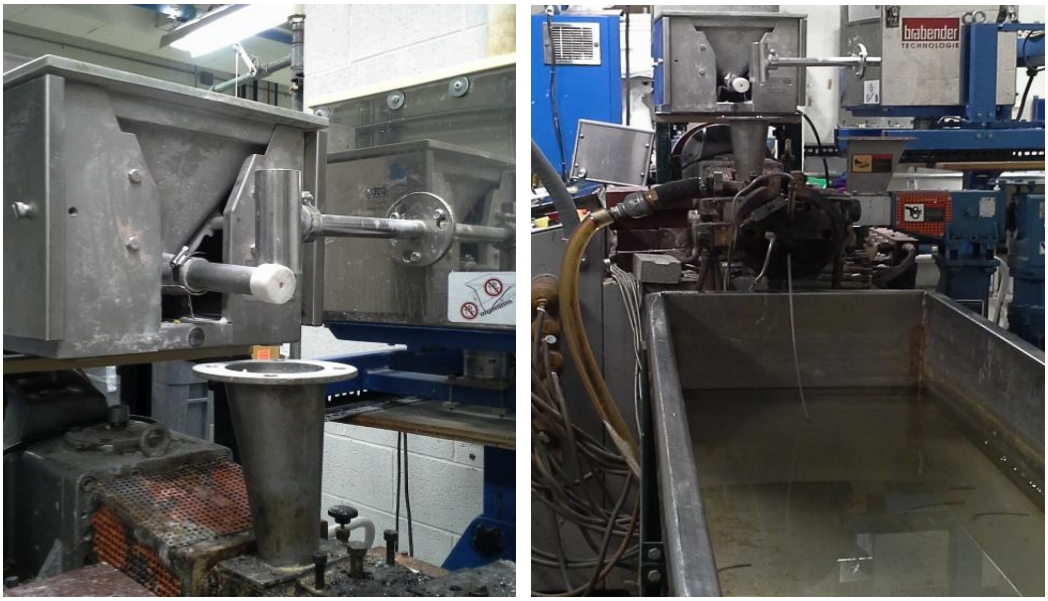

Figure 3.2 Master batch extrusion process: Left picture shows the feeder machine for PBAT resin and AOx. Right picture shows the water bath used to cool extruded filament

After obtaining the PBAM, PBPM and PBAC, a specific amount (presented in table 3.3) of pure PBAT resin was mixed with 20% PBAM, 20% PBPM and PBCM and were separately extruded in a Killion KLB 100 blown film extruder (Davis-Standard LLC, Pawcatuck, CT), respectively (Figure 3.3). The temperature profile of all film extrusion process was 177-182-182-177-177-162-154 ℃ for barrel zone 1, 2, 3, clamp ring, adapter, die 1 and 2, respectively [1]. A screw speed of 10 rpm and take up speed of 0.018m/s were used. During the production of the master batch and films, the heads and tails of each batch were discarded to obtain a homogeneous distribution of the AOx. The overall thickness of the produced PBC, PBA and PBP films for the treatments were 63.5 ± 5.1 µm (2.5±0.2 mil), 68.6 ± 2.5 µm (2.7±0.1 mil) and 76.2 ± 5.1µm (3.0±0.2 mil), respectively, which were measured by micrometer model 549M, Testing machine Inc. (N.Y., USA).

Table 3.3 Weight of master batch and PBAT resin used for producing the PBA, PBP and PBC film

	20% AOx –PBAT master bacth (g)	PBAT resin (g)
2% PBA	80	720
2% PBP	80	720
2% PBC	80	720

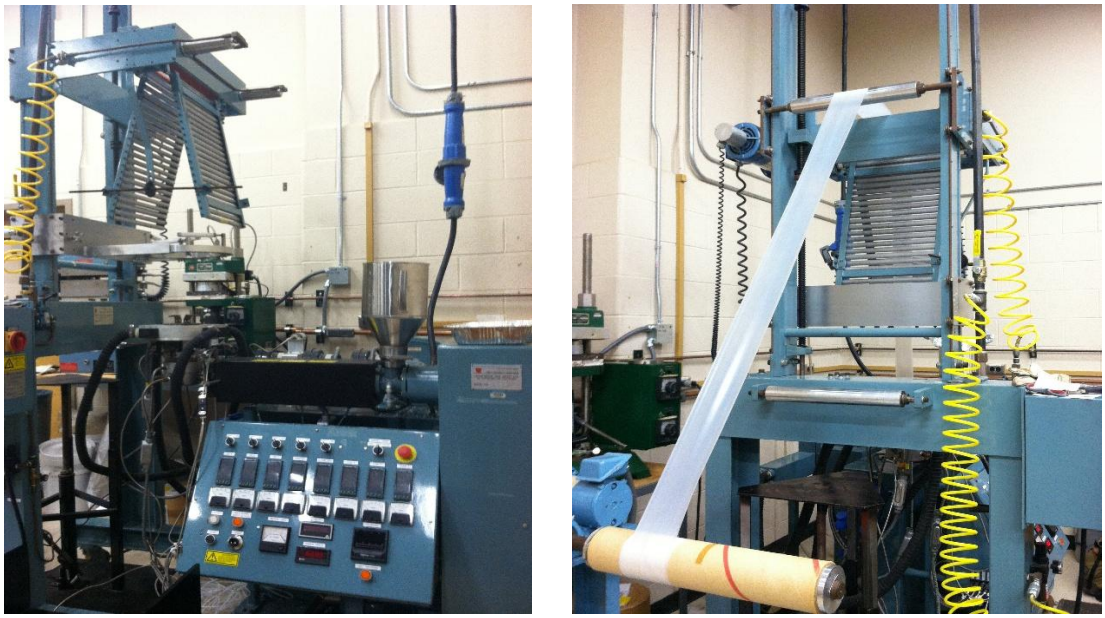

Figure 3.3 PBC, PBA and PBP blow film extrusion process: Left figure presents hopper, screw and blow film sections; Right figure presents reception of processed film.

3.2.3 Extraction and quantification of selected antioxidants for processed film

α-TOC and PG were extracted from the processed film (PBA and PBP) by stirring pieces of polymers (0.1 g) with 20 mL of methanol at 40 ℃ for 24 h in the dark. To protect the antioxidants from degradation during the extraction period, 100 µg/mL BHT was added to the solutions. Several extraction times were performed on the same material to ensure complete extraction of antioxidants. Three replicates were carried out. The amount of α-Tocopherol from the extruded films was quantified by using a high performance liquid chromatography (HPLC) (Waters model 2695, Milford, MA, USA) equipped with an auto sampler and a dual absorbance detector (Waters 2487) at 295 nm wavelength. Aliquots (10 µL) of the extraction were injected

into a C18 Nova-Pak column (3.9*150 mm; Waters) protected with a C18 guard column with run time of 12 min per injection. An isocratic elution of methanol - water (98:02) at 0.8 mL/min and 25 ℃- was used. Calibration curves from 0.2 to 10 µg/mL of α-TOC in methanol were carried out for qualification, R^2 was 0.99. Retention time for α-TOC was around 5.5 min and the limit of quantification (LOQ) was 0.1µg/mL.

The amount of PG from the extruded films was quantified by using a 3200 QTRAP® liquid chromatography-tandem mass spectrometry (LC/MS/MS) System (AB Sciex, Framingham, MA, USA) and a Shimadzu LC-20AD HPLC system and SIL HTc auto-sampler (Shimadzu Scientific Instruments, Addison, IL, USA). The instrument was operated by the Analyst® software. Aliquots (10 µL) of the extraction were injected into an Acenti® Express C18 column (2.1×50 mm; 2.7 µm particles) (Sigma-Aldrich, St. Louis, MO, USA) protected with a C18 guard column with run time of 7 min per injection. The temperature of the column was maintained at 40℃ via CTO-10A vp column oven. A gradient of 0.15% formic acid/ water (mobile phase A) and methanol (mobile phase B) at flow rate of 0.4 mL/min was set as follows: 95% A and 5% B was initial set and maintained for 0.5 min, then the ratio of 5% A and 95% B was reached in the following 2 min and kept this ratio from 2.5 to 5 min. Then a return to the initial settings (95% A and 5% B) was applied at 5.01 min and maintained at this proportion from 5.01 to 7 min. The samples were analyzed by electrospray ionization in negative mode (ESI-) and multiple reactions monitoring (MRM) (detail parameters presented in Table 3.4) by using a hybrid triple quadrupole linear ion trap ("Q-Trap"). Ion source settings for Gas 1 (nebulizer gas) and Gas 2(heater gas) were 10 and 10, respectively. Source temperature was 550℃. Ionspray voltage was set to -4500 V, curtain gas was set to 20 psi, and collision CAD gas was set to High mode. The results were analyzed by Analyst® software.

Table 3.4 MS parameters for the analysis of PG

	Q1 (amu)	Q3 (amu)	Dwell (s)	DP volt. (V)	Collision volt. (V)
PG	211.1	169	0.1	-60	-25

Calibration curves from 0.1 to 10 µg/mL of PG in methanol were carried out for quantification, R^2 was 0.96. Retention time for PG was 4.9 min and the limit of quantification (LOQ) was 0.01µg/mL.

3.2.4 Diffusion of antioxidants from processed film into food simulant.

The amount of antioxidants diffused from the process film into 95% ethanol was determined by using a migration cell according to ASTM D4754-11. The migration cell consisted of a 40 mL amber glass vial with a screw cap and silicon septum. Six round disc (2 cm in diameter) cut from the film were inserted in a stainless steel wire and placed in the amber vial containing 35 mL of 95% ethanol. Glass beads were used to separate each disc in order to expose both sides to liquid, which was displaced in Figure 3.4. A magnetic stirrer was used inside each vial to provide a constant agitation. The liquid volume/area ratio was 0.9 mL/cm^2 complying with ASTM D4754-11, which establishes a ratio between 155 and 0.31 mL/cm^2.

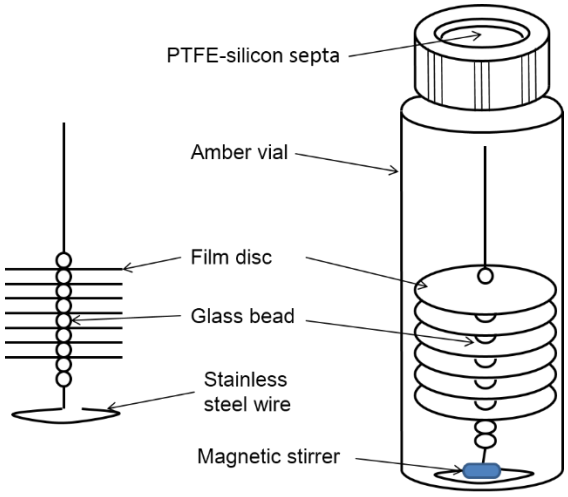

Figure 3.4 Migration test cell

3.2.4.1 Preliminary migration study

Preliminary migration studies were performed for processed PBA and PBP films into 95% ethanol. Two trials of PBA migration test at 40℃ and one trial of PBA migration test at 10, 20 and 30℃, respectively were done to get preliminary migration data to design the full migration experiment. Additionally, one trial of PBP migration test at 20 ℃ as conducted. Constant temperature chamber was used and controlled within ±0.5℃. A designed sample collection schedule was applied for each trial until equilibrium was reached. At each sample collection, 50 µL solution from the migration cell was diluted with 950 µL 95%ethanol. Then, the dilution solution was analyzed by HPLC for quantification. Antioxidants qualifications were performed as described in the extraction section. To establish the equilibrium stage for each temperature, the concentration (mg/L) versus time (s) of each vial at each temperature was plotted until the slope of the curve reached zero. Using the preliminary data, the scaled sensitivity coefficient (SSC) was obtained and an optimal experimental design (OED) was conducted to determine the sampling time interval for the final migration test.

3.2.4.2 Designed of the final migration test

According to the information obtained in the preliminary migration study, the final migration test for PBA and PBP were conducted at 10 ± 0.5, 20 ± 0.5 and 30 ± 0.5℃. Four cell replicates were used per each temperature. Samples were taken out periodically from each cell during 4 days for 10℃, 2 days for 20℃ and 2 days for 30℃. At each sampling time, 50 µL solution from migration cell was dilute with 950 µL 95%ethanol. Then the dilution solution was injected to HPLC for quantification. Antioxidants quantifications were performed as the same as described in extraction section.

3.2.5 Antioxidants release models

Migration processes for test conducted in migration cells are mostly described by standard Fick's law equations. Several types of boundary conditions are used to categorize solutions of the heat and mass (diffusion) equation. Five types of boundary conditions are defined at physical boundaries and a "zeroth" type defines the case with no physical boundaries. Table 3.5 shows the types of boundary conditions from numbers zero through five.

Table 3.5 Types of boundary conditions and associated number designation, adapted from (http://exact.unl.edu/exact/home/number.php)

Name of boundary condition	**Equation**	**Number**
No Physical boundary	T is bounded	0
Dirichlet	$T\|_{r_i} = f_i$	1
Neumann	$\frac{\partial T}{\partial n_i} = f_i$	2
Robin	$\frac{\partial T}{\partial n_i} + hT\|_{r_i} = f_i$	3
Thin, high-conductivity film	$\left[k\frac{\partial T}{\partial n_i} + (\rho cb)\frac{\partial T}{\partial t}\right]_{r_i} = f_i$	4
Thin, high-conductivity film with addition of convection	$[\mathrm{k}\frac{\partial T}{\partial n_i} + (\rho cb)\frac{\partial T}{\partial t} + hT]_{r_i} = f_i$	5

Type 1 is called the Dirichlet condition or referred to as a fixed boundary condition. It corresponds to the situation for which the surface is maintained at a fixed temperature in heat transfer. Type 2 is called the Neumann condition, which describes the existence of a fixed or constant heat flux at the surface. Type 3 is called the Robin condition, sometimes called convective boundary conditions. It corresponds to the existence of convection heating (cooling)

at surface. Type 4 represents a thin, high-conductivity film at the body surface. Type 5 represents a thin, high-conductivity film at the body surface with the addition of convection heat losses from the surface. Type 0 is used to identify the case with no physical boundary exists.

In this study, the migration process occurred between well-mixed food simulant and packaging material with well-distributed AOx. The mass transfer resistance on the side of food can be negligible. Before migration process happen, the concentration of AOx in the packaging material equals to the initial concentration and the concentration of AOx in food simulant is 0. When migration occurs, the amount of AOx migrated from packaging material is the same amount existing in food simulant. Then, boundary conditions type 3 or 4 mentioned above can be used to solve the studied migration. According to Fick's second law equation for D, two analytical solutions were applicable for this experiment conducted in one-dimension, and they are expressed by equation 3.6 and equation 3.9 [2, 3]. When the diffusion is in one-dimension and in a limited volume of film is in contact with a finite volume of solution, equation 3.6 is used.

$$\frac{M_t}{M_\infty} = 1 - \sum_{n=1}^{\infty} \frac{2\alpha(1+\alpha)}{1+\alpha+\alpha^2 q_n^2} \exp\left(-\frac{D q_n^2 t}{l^2}\right) \qquad 3.6$$

where M_t/M_∞ is the concentration of the antioxidant diffused at time t divided by the concentration of the antioxidant diffused at equilibrium; l is the thickness of the film and the q_n are the non-zero positive roots of tan $q_n = \alpha q_n$ and α is expressed in 3.7:

$$\alpha = \frac{V_S}{V_P \cdot K_{P,S}} \qquad 3.7$$

where V_S and V_P are the molar volume of the simulant and the polymer. $K_{P,S}$ is the partition coefficient of antioxidant between PBAT and the simulant, which can be calculated from the ratio of the concentration of the antioxidant in the PBAT film ($C_{P,\infty}$) and the simulant ($C_{S,\infty}$) at equilibrium according to following equation:

$$K_{P,S} = \frac{C_{P,\infty}}{C_{S,\infty}} \quad 3.8$$

When the amount of simulant can be considered infinite (i.e., $\alpha \gg 1$ since $V_S \gg V_P$ and /or $K_{P,S} < 1$), equation 3.9 is used

$$\frac{M_t}{M_\infty} = 1 - \frac{8}{\pi^2}\sum_{m=1}^{\infty}\frac{1}{(2m+1)^2}\exp\left(-\frac{D(2m+1)^2\pi^2 t}{l^2}\right) \quad 3.9$$

Diffusion coefficients (D, cm^2/s) were calculated for each antioxidant at different experimental temperatures. The value of D was determined by minimizing the sum of the squares errors (SSE) of the measured and estimated values. To determine the fit of the experimental data to equation 3.6 and/or 3.9, a nonlinear regression (nlinfit) function in MATLAB R2011b (MathWorks, Natick, MA, USA) was applied to the data [4].

3.2.6 Activation energy for the diffusion (Ea) of selected antioxidants into food simulant

To determine the effect of temperature on the diffusion of α-Tocopherol and propyl gallate from PBAT films into 95% ethanol, the activation energy (E_a) was calculated using the Arrhenius equation:

$$\mathrm{D} = D_0 e^{\left[-\frac{E_a}{R}T\right]} \quad 3.10$$

where D is the diffusion coefficient, D_0 is the pre-exponential factor of diffusion, E_a is the activation energy of diffusion, R is the ideal gas constant (8.3145 J/Kmol), and T is the temperature in K. E_a was obtained from the slope of a plot of the reciprocal of temperature (*1/T*) vs the logarithm of D (E_a= - slope×2.303R) [5].

3.2.7 Optical properties

The transmission to UV-visible light through the films was measured with a Perkin-Elmer Lambda 25, UV-visible spectrophotometer (Perkin-Elmer Instruments, Beaconsfield, UK) between 190 and 800 nm at a rate of 480 nm/min, a slit width of 1.0 nm and an interval of 1.0

nm. An integrating reflectance spectroscopy accessory (model RSA-E-20, Labsphere®, North Sulton, NH) was also employed.

Films color was determined by a LabScan XE (HunterLab, Reston, VA, USA). The Hunter L*, a*, b* values were obtained by analysis software Easymatch QC version 3.8. Three replicates for each type of film were measured. Total difference in color ΔE was calculated as expressed in equation 3.12:

$$\Delta E = \sqrt{\Delta L^2 + \Delta a^2 + \Delta b^2} \qquad 3.12$$

where $\Delta L = L_{PBATANTIOXISANT} - L_{PBAT}$, $\Delta a = a_{PBATANTIOXIDANT} - a_{PBAT}$, $\Delta b = b_{PBATANTIOXIDANT} - b_{PBAT}$

3.2.8 Statistic analysis

One-way analysis of variance (ANOVA) was used to analyze the data. Comparisons of experimental data were conducted by using Tukey‘s HSD test with 95% level of confidence (α=0.05). Statistical software SAS (Version 9.4, SAS Institute Inc., Cary, NC, US) was used

REFERENCES

REFERENCES

1. Chidambarakumar, M., et al., *Biodegradable polymeric nanocomposite compositions particularly for packaging*. 2009, Google Patents.

2. Crank, J., *The mathematics of diffusion*. 1979: Oxford university press.

3. Manzanarez-López, F., et al., *Release of α-Tocopherol from Poly (lactic acid) films, and its effect on the oxidative stability of soybean oil.* Journal of Food Engineering, 2011. **104**(4): p. 508-517.

4. Dhoot, G., et al., *Determination of eugenol diffusion through LLDPE using FTIR-ATR flow cell and HPLC techniques.* Polymer, 2009. **50**(6): p. 1470-1482.

5. Limm, W. and H.C. Hollifield, *Modelling of additive diffusion in polyolefins.* Food Additives & Contaminants, 1996. **13**(8): p. 949-967.

CHAPTER 4 RESULTS AND DISCUSSIONS

4.1 Hansen Solubility parameters determined by the experimental method

The Hansen solubility parameters (HSPs) of PBAT were determined by an experimental method as described in section 3.2. The scores for the 17 solvents are listed in table 4.1.

Table 4.1 Scoring of PBAT in various solvents after two days of storage

Solvent Number	IUPAC Name & (CAS Number)	Solvent	Score
1	Dichloromethane (75-09-2)	Dichloromethane	1
2	Methylbenzene (108-88-3)	Toluene	3
3	1,1,2,2-Tetrachlorethane (79-34-5)	Tetrachloroethane	2
4	Butan-2-one (78-93-3)	Methyl Ethyl Ketone	3
5	Cyclohexane (110-82-7)	Cyclohexane	6
6	(2-hydroxyethoxy) ethan-2-ol(111-46-6)	Diethylene Glycol	6
7	Chloroform (67-66-3)	Chloroform	1
8	Propanone (67-64-1)	Acetone	4
9	Oxacyclopentane (105-99-9)	THF	1
10	Acetonitrile (75-05-8)	Acetonitrile	4
11	Dimethyl Sulfoxide (67-68-5)	Dimethyl Sulfoxide	6
12	Ethyl Acetate (141-78-6)	Ethyl Acetate	5
13	Methanol (67-56-1)	Methanol	5
14	Hydroxybenzene (108-95-2)	Phenol	2
15	N,N-dimethylmethanamide (68-12-2)	DMF	3
16	Hexane (110-54-3)	Hexane	6
17	Ethanol (64-17-5)	Ethanol	6

Figure 4.1 shows that PBAT was completely dissolved in dichloro methane, chloroform and THF after 15 min of sonication, but not in tetrachloro ethane and phenol solvents, which took two days of storage for PBAT to dissolve. According to these observations, a score of 1 was given to dichloro methane, chloroform and THF, and a score 2 was given to the tetra chloroethane and phenol solvents.

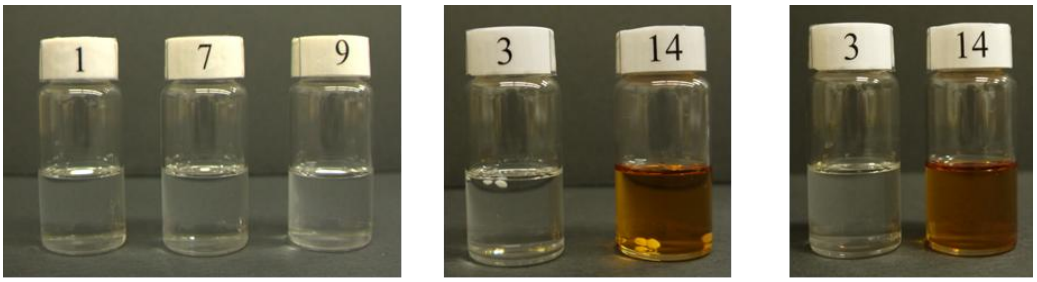

Figure 4.1 Dissolution of PBAT in dichloromethane, chloroform, THF, tetrachloroethane and phenol (a- left to right: 1-dichloromethane, 7- chloroform, and 9-THF, b-PBAT in 3-tetrachloroethane and 14-phenol after 15 min of sonication, c-PBAT in 3-tetrachloroethane and 14-phenol after two days of storage) (For the better visualization of this dissolution phenomenon, the reader is suggested to view the electronic version of this document)

The dissolution behavior of PBAT pellets in other solvents such as toluene, methyl ethyl ketone, DMF, acetone, acetonitrile, ethyl acetate and methanol did not vary very much after 15 min of sonication and 2 days of storage. PBAT was not dissolved completely in these solvents, instead it settled down to the bottom, or swelled with different levels when settled. Also, it gelled at some point. PBAT was swelled most in toluene, methyl ethyl ketone and DMF, and form gell. Then, a score of 3 was given for these three solvents. Swelling of PBAT in acetone, acetonitrile, ethyl acetate and methanol was less than that in the former solvents. Meanwhile PBAT in cyclohexane, diethylene glycol, dimethyl sulfoxide, hexane and ethanol did not change much comparing to the previous mentioned solvent. The scores were graded based on the interaction between PBAT and the solvents. Figure 4.2 and 4.3 indicate how PBAT was dispersed in various solvents after 15 min of sonication and two days of storage, respectively. PBAT pellet was used in the experimental method to measure HSPs instead of PBAT film, since HSPs of pellets and films are assumed the same since the geometry and chemical structures are not changing. So, based on the group contribution calculation methods, their HSPs should be the same.

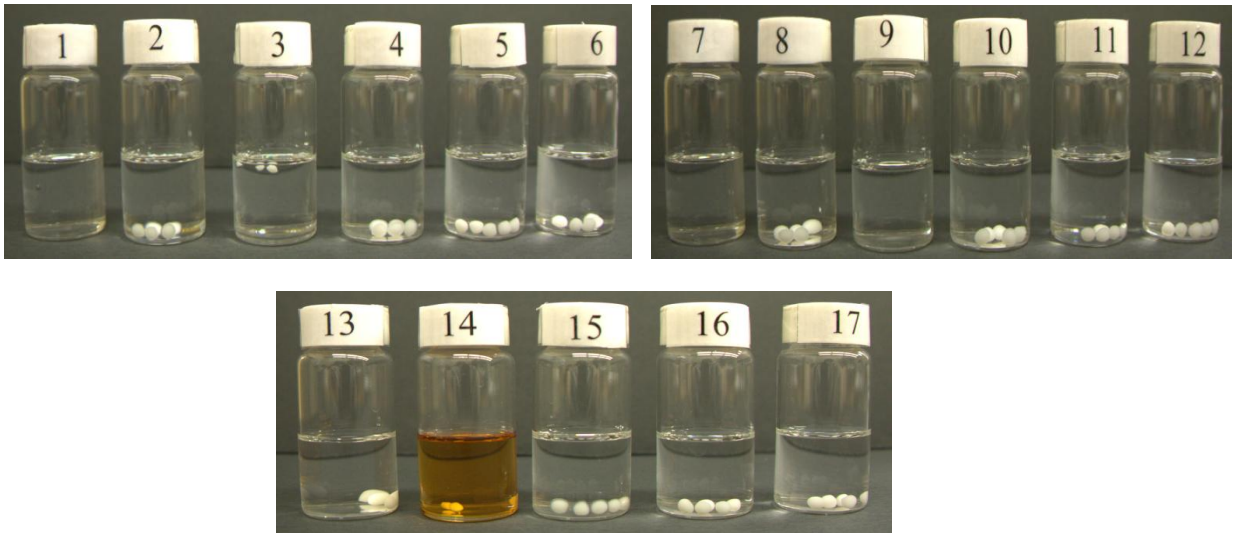

Figure 4.2 Dissolution of PBAT in various solvents after 15 min sonication (from left to right, named number 1-17: 1-dichloro methane, 2-toluene, 3-tetra chloro ethane, 4-methyl ethyl ketone, 5-cyclohexane, 6-diethylene glycol, 7-chloroform, 8-acetone, 9-THF, 10-acetonitrile, 11-dimethyl sulfoxide, 12-ethyl acetate, 13-methanol, 14-phenol, 15-DMF, 16-hexane, 17-ethanol)

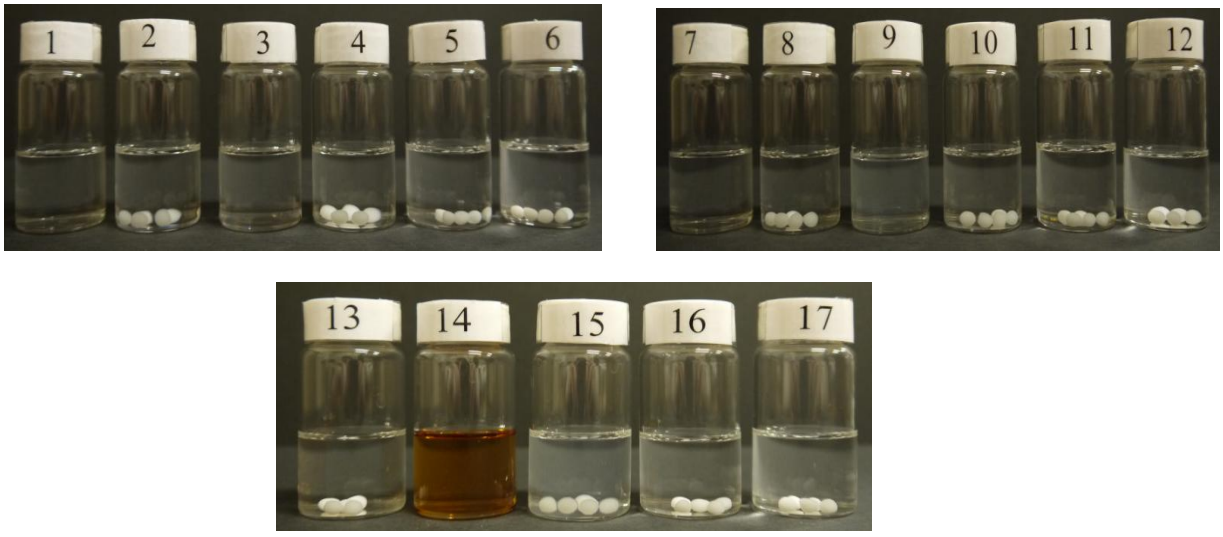

Figure 4.3 Dissolution of PBAT in various solvents after two days storage (from left to right, named number 1-17: 1-dichloro methane, 2-toluene, 3-tetra chloro ethane, 4-methyl ethyl ketone, 5-cyclohexane, 6-diethylene glycol, 7-chloroform, 8-acetone, 9-THF, 10-acetonitrile, 11-dimethyl sulfoxide, 12-ethyl acetate, 13-methanol, 14-phenol, 15-DMF, 16-hexane, 17-ethanol)

The HSPiP® software (Horsholm, Denmark) was used to estimate the HSPs values of PBAT based on the data from Table 4.1 obtained by dissolving PBAT in the 17 mentioned solvents. Table 3.1 provided in chapter 3 lists the unique dispersion, polar and hydrogen forces

values for each solvent. These data were input into the HSPiP® software to obtain the dispersion, polar, hydrogen forces and interaction radius of PBAT as shown in Table 4.2. The HSPiP® software used the scores define for each solvent to fit a sphere of PBAT in the HSP space, which allows good solvents to be located inside the sphere and bad solvents outside [1, 2]. The calculation indicates that the HSP of PBAT are 18.97, 9.83 and 9.10 (δ_d, δ_p and δ_h respectively) and the radius of dissolution is 3.9, which means that a wide rage of solvents located in or on this sphere will dissolve, interact or at least swell PBAT. The solvents close to the center of the sphere are more likely to totally dissolve the polymer.

Table 4.2 Dispersion, polar, hydrogen parameters and interaction radius for PBAT

Material	**Dispersion δ_d(MPa $^{1/2}$)**	**Polar δ_p(MPa $^{1/2}$)**	**Hydrogen Force δ_h(MPa $^{1/2}$)**	**Interation Radius (R_o)**
PBAT	18.97±0.3	4.83±0.75	9.10±0.3	3.9

4.2 Hoftyzer and Van-Krevelen theoretical calculation method

The HSP parameters of two biodegradable polymers and twenty-five antioxidants were predicted according to the Hoftyzer and Van-Krevelen methods. Butylated hydroxytoluene (BHT) is next used as an example to explain how to use the Hoftyzer and Van-Krevelen methods was used to calculate the HSP. Figure 4.4 shows the chemical structure for BHT.

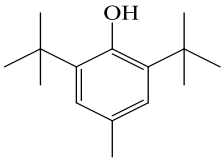

Figure 4.4 BHT chemical structures

The BHT chemical structure can be broken down in four parts, which are seven –CH_3, one –OH, two –C and one benzene ring. Based on Table 4.3 [3], the group contributions values of F_{di}, F_{pi} and E_{hi} can be found for each structural group. The sum of F_{di}, F_{pi} and E_{hi} can be calculated based on the types and number of structural groups present on BHT. Table 4.4

summarizes the values of F_{di}, F_{pi} and E_{hi} for BHT. Table 4.4 shows the detailed calculation for generating the HSPs of BHT. The molar volume for BHT is 244.3 cm^3/mol [4].

Table 4.3 Solubility parameter components according to the group contribution method of Hoftyzer-Van Krevele**.**

Structural group	*Fdi* ($J^{1/2} \cdot cm^{3/2} \cdot mol^{-1}$)	*Fpi* ($J^{1/2} \cdot cm^{3/2} \cdot mol^{-1}$)	*Ehi* (J/mol)
-CH_3	420	0	0
-CH_2-	270	0	0
	80	0	0
	-70	0	0
	400	0	0
	200	0	0
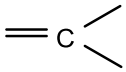	70	0	0
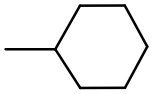	1620	0	0
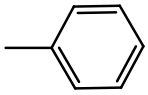	1430	110	0
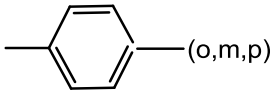	1270	110	0
—F	(220)	-	-
—Cl	450	550	400
—Br	(550)	-	-
—CN	430	1100	2500
—OH	210	500	20000
—O—	100	400	3000
—COH	470	800	4500
—CO—	290	770	2000
—COOH	530	420	10000
—COO—	390	490	7000
HCOO—	530	-	-
—NH_2	280	-	8400
—NH—	160	210	3100
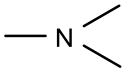	20	800	5000
—NO_2	500	1070	1500
—S—	440	-	-
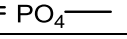	740	1890	13000
ring	190	-	-

Table 4.3 (cont'd)

Structural group	*Fdi* ($J^{1/2} \cdot cm^{3/2} \cdot mol^{-1}$)	*Fpi* ($J^{1/2} \cdot cm^{3/2} \cdot mol^{-1}$)	*Ehi* (J/mol)
One plane of symmetry	-	0.5×	-
Two plane of symmery	-	0.25×	-
More plane of symmery	-	0	0×

Table 4.4 Addition of the group contributions for BHT

The group contributions	Numbers	F_{di} (J $^{1/2}$.cm$^{3/2}$/mol)	$F_{pi}{}^2$ (J $^{1/2}$.cm$^{3/2}$/mol)	E_i (J /mol)
-CH_3	7	2940	0	0
-OH	1	210	250000	20000
-C-	2	-140	0	0*2
Benzene	1	1270	12100	0
Total		4280	262100	20000

According to equations (3.3) to (3.5) in chapter 3 and table 4.4:

$$\delta_d = \frac{\sum F_{di}}{V} = \frac{4280}{244.3} = 17.52 \text{ J}^{1/2}/\text{cm}^{3/2} = 17.52 \text{ MPa}^{1/2}$$

$$\delta_p = \frac{\sqrt{\sum F_{pi}^2}}{V} = \frac{\sqrt{262100}}{244.3} = 2.10 \text{ J}^{1/2}/\text{cm}^{3/2} = 2.10 \text{ MPa}^{1/2}$$

$$\delta_h = \sqrt{\frac{\sum E_{hi}}{V}} = \sqrt{\frac{20000}{244.3}} = 0.58 \text{ J}^{1/2}/\text{cm}^{3/2} = 0.58 \text{ MPa}^{1/2}$$

The three solubility parameter components (δ_d, δ_p and δ_h) for BHT are 17.52 MPa $^{1/2}$, 2.10 MPa $^{1/2}$ and 0.58 MPa ^{½}, respectively.

Table 4.5 lists the HSP values for 25 antioxidants, two biodegradable polymers and the solvents studied.

Table 4.5 Summary of HSPs for the polymers, solvents and antioxidants studied

Category	Material	δ_d(MPa $^{1/2}$)	δ_p(MPa $^{1/2}$)	δ_h(MPa $^{1/2}$)
Polymer	PLA	18.9	0.73	10.3
	PBAT	18.5	4.9	7.8
Solvent	Ethanol	15.8	8.8	19.4
	Water	15.5	16	42.3
Antioxidants	BHT	17.5	2.1	0.58
	Ascorbic acid	10.2	7.5	22.0
	Catechin	13.3	4.5	19.7
	Quercetin	23.0	15.8	25.0
	Octyl gallate	18.2	6.9	1.0
	Dodecyl gallate	17.8	5.4	0.79
	TBHQ	51.5	10.5	1.9
	Ralox 35	17.1	3.0	9.3
	Irganox 1135	18.5	2.6	8.1
	Irganox 1076	18.6	1.9	6.9
	Nordihydroguaiaretic acid	18.63	0.13	1.07
	Epicatechin gallate	15.1	4.3	8.5
	Epigallocatechin gallate	14.3	3.6	20.4
	Epigallocatehin	13.7	4.7	21.1
	Propyl gallate	19.2	7.3	19.6
	2,3,5-trihydroxybutyrophenone	19.6	7.2	19.6
	Butylated hydroxyanisole	17.3	2.8	11.2
	4-Hydroxymethyl-2,6-di-tert-butylphenol	15.7	2.9	9.1
	α-tocopherol	15.01	1.41	7.12
	Resveratrol	21.26	9.03	10.91
	Rutin	19.3	16.1	25.4
	Astaxathin	16.3	3.3	8.9
	Lycopene	15.6	0.0	0.0
	β-carotene	15.47	0.0	0.0
	Melatonin	18.6	0.2	5.8

4.3 Analysis of HSP parameters

The HSP values of PBAT were obtained by the experimental method and the Hoftyzer and Van-Krevelen calculation procedure. Table 4.6 presents the data from these two methods. The values for the three components of the HSP were found to be very similar to each other according to these two different methods of calculation. In this study, the data from the experimental method

was then used. Large variation in δ_h is normal due to the unpredictable nature of the chance of forming hydrogen bonds.

Table 4.6 HSP for PBAT from two methods

PBAT	δ_d(MPa $^{1/2}$)	δ_p(MPa $^{1/2}$)	δ_h(MPa $^{1/2}$)
Experiment method	18.47±0.3	4.83±0.75	9.10±0.3
Calculation method	18.55	4.90	7.82

Base on the basic principle of HSP- "like dissolves like", the distance between two different materials can be estimated by the affinity between them. The greater the distance between the two materials, the less alike they are. Figure 4.5 shows a 3D plot of all HSPs of the antioxidants, polymers and solvents and their relative positions in the Hansen space.

According to the information provided by the 3D plot, there are some antioxidants located close to the sphere of interaction of ethanol, while others are presenting closer to the sphere of PBAT and PLA. In this study, PBAT was selected as the main studied polymeric material. So, a zoom out of the 3D plot is displayed in Figure 4.6. Only the sphere of water, ethanol, PBAT and the antioxidants around or located in the sphere of ethanol and/or PBAT are plotted. Four antioxidants, named in the graph propyl gallate (PG) and ascorbic acid (AA) around the sphere of ethanol, and Irganox 1076 (IR1076) and α-tocopherol (α-TOC) around the sphere of PBAT are individually marked. Based on the HSP methodology and the graph, PG and AA have higher affinity to ethanol comparing to IR 1076 and α-TOC. IR 1076 and α-TOC have higher affinity to PBAT than PG and AA. So, one antioxidant close to PBAT (*i.e.*, inside the interaction regions of polymer) - α-TOC and one antioxidant close to ethanol (*i.e.*, inside the interaction regions of the solvent) -PG were selected and later on incorporated into PBAT. Migration test in 95% ethanol were conducted for these antioxidants to verify the initial estimation that PG incorporated in PBAT will have higher affinity towards ethanol than α-TOC.

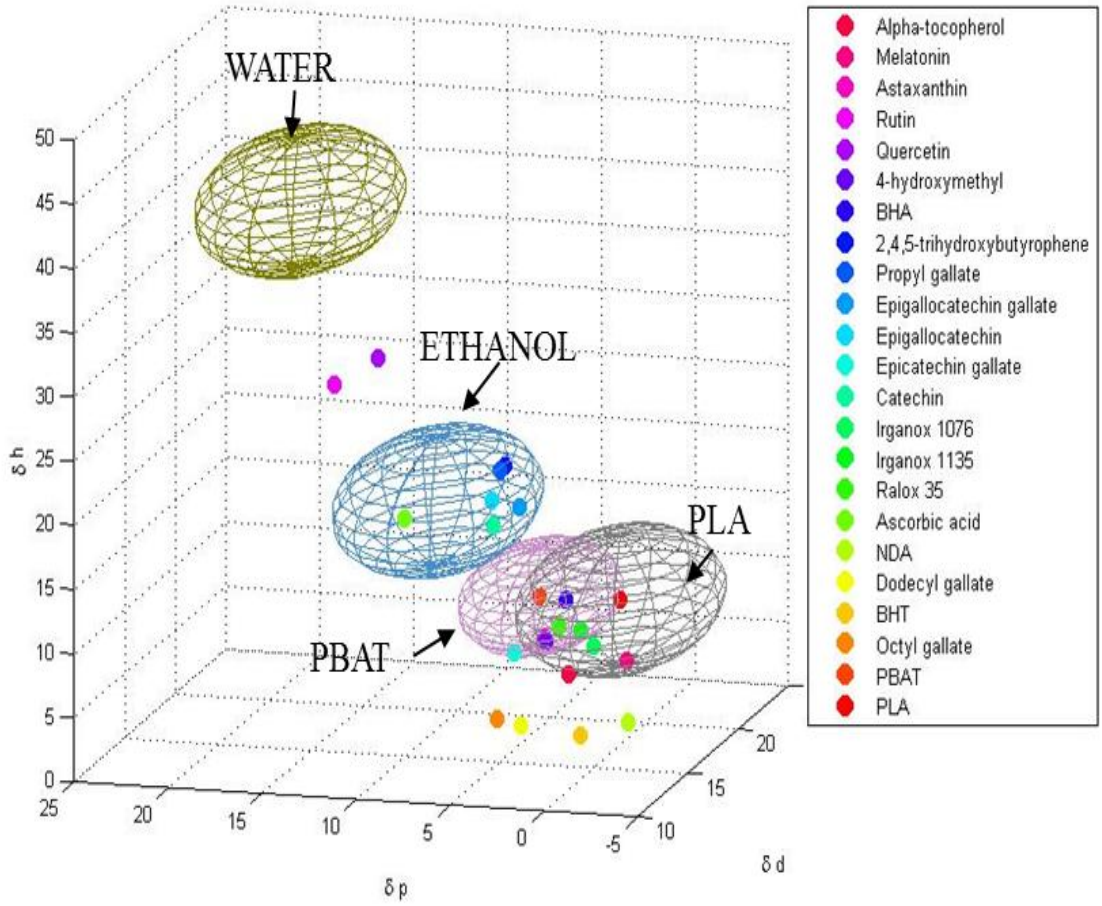

Figure 4.5 3D plot of the HSP parameters for the 25 antioxidants, 2 biodegradable polymers and water and ethanol. The spheres show the radius of interaction of the solvents and the polymers**.**

To further justify the selection of one antioxidant among PG, AA, IR 1076 and α-TOC, their information is listed in Table 4.7. Between PG and AA, which are close to the sphere of ethanol, the antioxidant capacity of PG is greater than that of AA according to DPPH measurement of the antioxidant capacities [5]. The reference used the IC_{50} to indicate the antioxidant capacity. The IC_{50} values for AA and PG were 11.8 µM and 4.4 µM in methanol and 11.5 µM and 4.7 µM in buffered methanol as reaction medium, respectively. While in the case of IR 1076 and α-TOC, which is close to sphere of interaction of PBAT, the antioxidants capacity of α-TOC is greater than that of IR 1076 [6]. Samples containing α-TOC have higher level of

retention of parent antioxidant than that for IR 1076 through HPLC analysis of dichloromethane extracts of polymer samples. So, PG and α-TOC were selected and procured for this study.

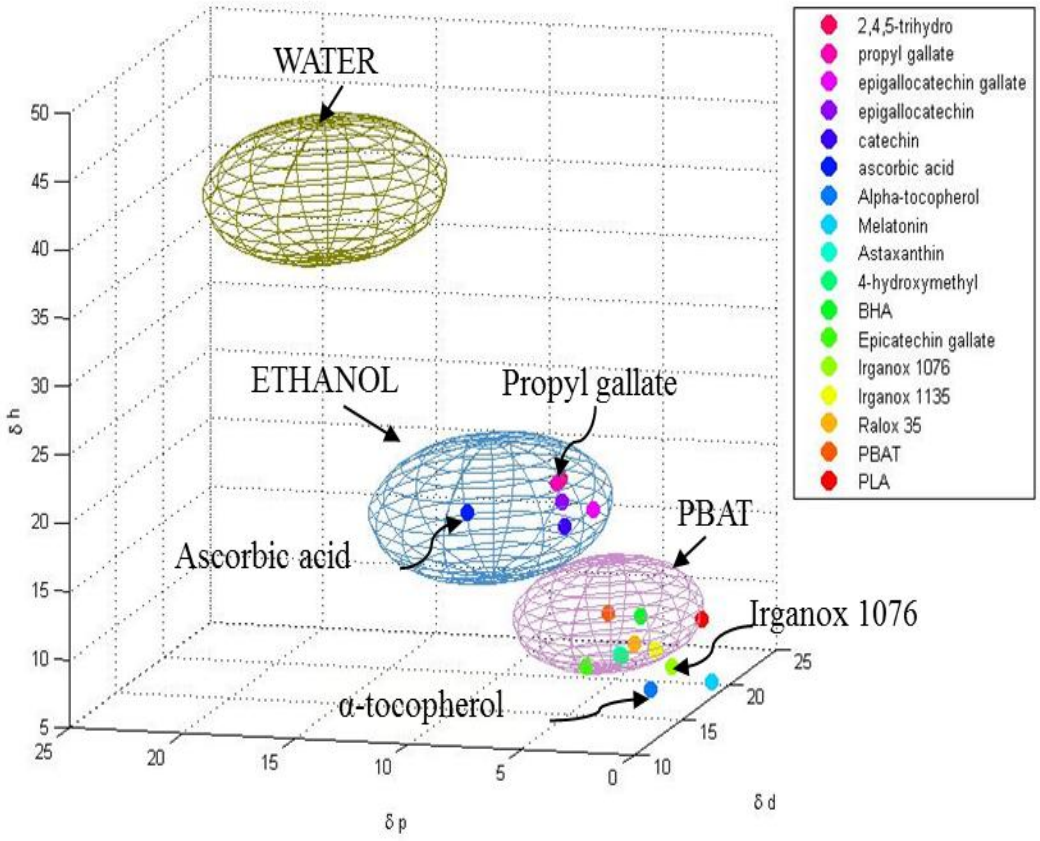

Figure 4.6 3D plot of selected HSP parameters

Table 4.7 Information summary for selected antioxidants

Antioxidants	**Molar volume(cm^3/mol)**	**Density(g/cm^3)**	T_D^* (℃)	**Melting point** (℃)
PG[1]	169.7	1.25	214	150
AA[2]	176.1	1.65	220 [7]	190-192
IR 1076[3]	453.38	1.01	230 [8]	50-55
α-TOC[4]	528	0.95	241	2.5-3.5

Note: * T_D= thermal decomposition point;
1 the information was provided by Sigma Aldrich where PG bought and referred to Wikipedia.
2 the information was referred to Wikipedia.
3 the information was referred to Wikipedia.
4 the information was provided by Sigma Aldrich where PG bought and referred to Wikipedia.

4.4 Quantification of α-TOC and PG after film processing

The final concentrations of α-TOC and PG in their master batch added with 20% wt/wt of the antioxidants were 17.3 ± 0.4% and 17.8 ± 0.0%, respectively. The loss of α-TOC and PG during the processing of PBAM and PBPM were 13.5 ± 0.4% and 11.0 ± 0.0% respectively. The final concentrations of α-TOC and PG in the produced cast film were 1.5 ± 0.0 % and 1.8 ± 0.05 %, respectively. The loss of antioxidant during processing was expected and attributed to several aspects. Since α-TOC is a stickier liquid, some α-TOC in a prepared mixture of α-TOC with PBAT was obviously left in the container during the master batch process. While PG is obtained as powder, so it is better handled when introduced to the extruder. During the master batch production and film processing, the material was poured into the feeder of the master batch extruder at 110℃ and at 177℃ in the feeder of blow film extruder. For both processes, the material took 5 to 10 min to come out from the feeder to the die, so a large friction was applied between the barrel and the screw. Additionally, in the stage of pelletization and film production process, it is normal cause that the AOxs present in matrix to degrade [9, 10]. Adherence of antioxidants to the screw and the barrel could also contribute to further loss of the antioxidants. Manzanare et al. also reported similar loss of α-TOC for production of poly (lactic acid) (PLLA) compounded with α-TOC [11].

Table 4.8 Concentrations of antioxidants in the film after film processed

Films	Antioxidant (w %)	
	Before extrusion	After extrusion
PBP	1.78	1.8±0.05
PBA	1.73	1.5±0.01

4.5 Migration of α-TOC and PG into food simulant (95% ethanol)

4.5.1 Preliminary migration study

Initial migration studies were conducted to determine the sampling interval needed to conduct the migration test. Sampling interval time (every 30 min in the first 3 h) was used for one trial of PBA migration test at 40℃. The equilibrium (steady state) of migration of α-TOC was reached at 30 min of the study indicating a very fast diffusion of α-TOC from PBAT. There was not obvious change of peak area of the analyzed solution detected by HPLC from the first sampling time until 24 h. An adjusted sample collection schedule every 5 min for 35 min at the beginning of the migration test was applied. The data for this adjusted test confirmed that migration of PBA in 95% ethanol reached equilibrium after 30 min. PBA migration into 95% ethanol at 40℃ was too fast to determine the unsteady state. One trial of PBA migration at 30, 20, and 10℃, respectively and one trial of PBP at 20℃ were done at designed sampling time. The data from all these trials were analyzed by determining the scaled sensitivity coefficient (SSC), by MATLAB R2011b (MathWorks, Natick, MA, USA) provided by Samsudin *et al* [12]. SSC are needed to determine whether the migration parameters can be estimated with relative smallest error. To scale of the sensitivity coefficient, it is obtained by multiplying the sensitivity coefficient with its respective parameters (Equation 4.1). SSC plots was used to determine the correlation among the main parameters studied in this research [13]. The red line in Figure 4.7 stands for M_∞ and the blue line stands for the D. In Figure 4.7 a to d can easily be seen that the behavior of the red line and blue line are different, and that these two parameters are not correlated and can be determined simultaneously for the same experiment. The SSC plot also provides important timing information to design the full migration experiment. Taking PBA migration trial at 10℃ as an example, the blue line is increasing to reach a maximum peak from

time 0 to 1.4 h. So during this period more sampling points should be collected to guarantee a proper estimation of *D*. After this time period, less frequent sampling points can be taken. Based on the plot, a timing table was created for conducting the final migration test. Table 4.9 shows an example for PBA final migration test at 10℃. Then the final migration test for PBA and PBP were conducted according to the timing table created based on SSC.

$$X'_D = D\frac{\partial_\eta}{\partial_D} \qquad 4.1$$

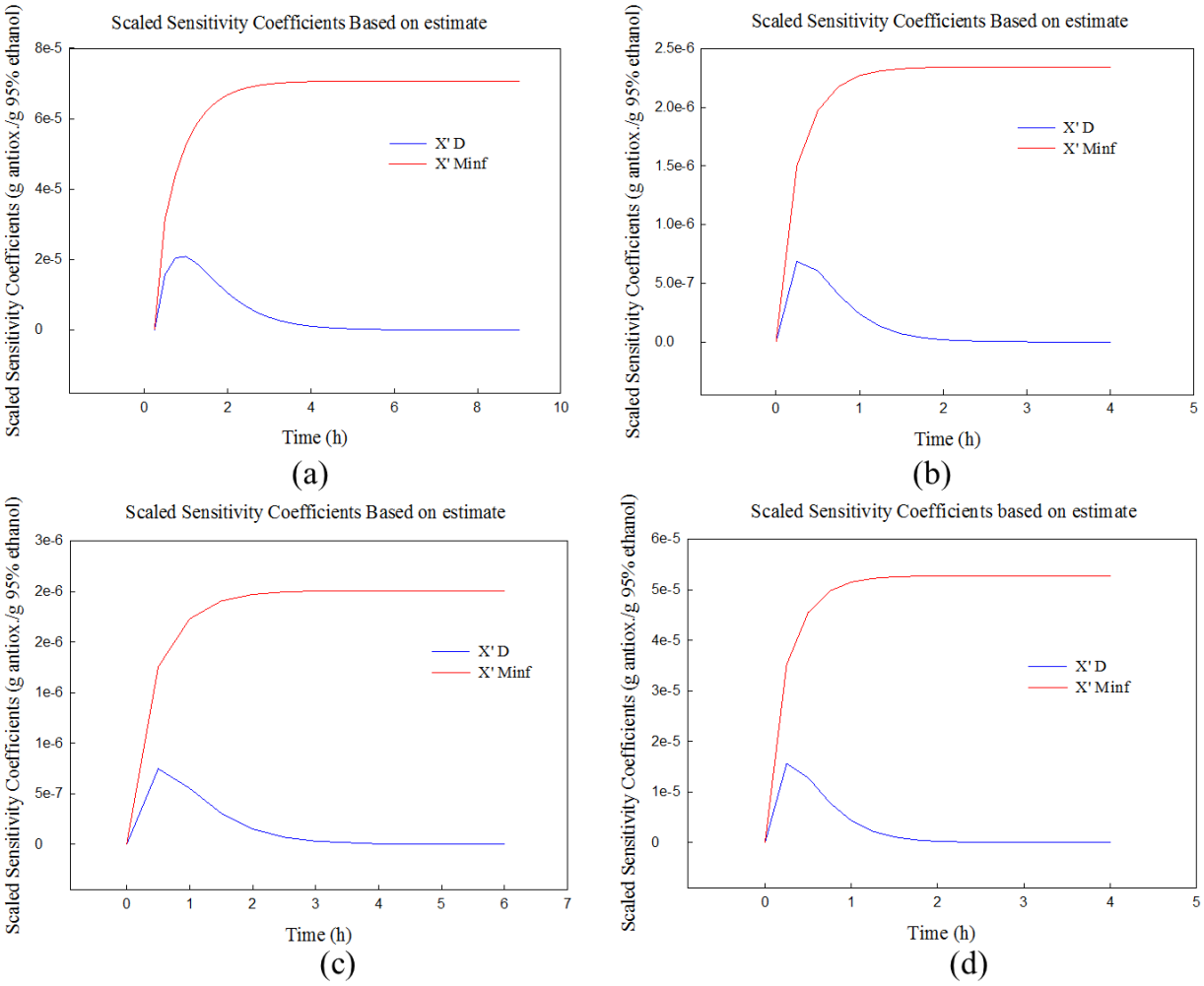

Figure 4.7 Scaled sensitivity coefficient plot for PBA migration trial at 30, 20, and 10℃ and PBP migration trial at 20℃ : (a) PBA migration trial at 10℃, (b) PBA migration trial at 20℃, (c) PBA migration trial at 30℃, (d) PBP migration trial at 20℃

Table 4.9 Timing table for PBA final migration test at 10℃

No.		Vial 1	Vial 2	Vial 3	Vial 4
	Time (h)	Time (min)	Time (min)	Time (min)	Time (min)
1	0.25	15	17.5	20	22.5
2		30	32.5	35	37.5
3		45	47.5	50	52.5
4	1	60	62.5	65	67.5
5		75	77.5	80	82.5
6		90	92.5	95	97.5
7		105	107.5	110	112.5
8	2	120	122.5	125	127.5
9	3	180	182.5	185	187.5
10	4	240	242.5	245	247.5
11	6	360	362.5	365	367.5
12	8	480	482.5	485	487.5
13	12	720	722.5	725	727.5
14	27	1620	1622.5	1625	1627.5
15	41	2460	2462.5	2465	2467.5

4.5.2 Final migration study

In the experimental migration of α-TOC and PG from PBAT films to 95% ethanol at 10, 20, and 30℃, the diffusion of both antioxidants showed a typical Fick's behavior. Equilibrium at 10, 20, and 30℃ was obtained for both PBA film and PBP film at 1.75 h, 1 h and 0.75 h, respectively. The experiments were stopped at 2 d for 10℃, 1 d for 20℃ and 1 d for 30℃, as designed according to the preliminary study. At the end of the experiment, the total release of α-TOC was 99.63, 99.63 and 99.62% at 10, 20, and 30℃, respectively while the release of PG was 99.26, 99.46 and 99.21% at 10℃, 20, and 30℃. At each temperature, almost a total migration of α-TOC and PG was observed (>99%) at a fast rate. $K_{P,S}$ at the three temperatures for PBA and PBP were determined and shown in table 4.10. The $K_{P,S}$ value was calculated from the ratio of the concentration of the antioxidant left in the film ($C_{P,\infty}$) and the concentration of antioxidants in the simulant ($C_{S,\infty}$) at equilibrium. $K_{P,S}$ >1 indicates a higher concentration of migrant in the polymer compared to that in the solvent at steady state [14]. In this study, $K_{P,S}$ for α-TOC at the

three temperatures were all less than 1 and not significantly different was found among them. Values of $K_{P,S}$ for PG were slightly above 1, there was no significant difference between them. The low $K_{P,S}$ values at each temperature for both α-TOC and PG agreed with the release of more than 99% α-TOC and PG into 95% ethanol. Also the low $K_{P,S}$ values indicated that α-TOC and PG migration systems can be considered and solved with the Fickian's equation for an infinite simulant volume [15] [16], as expressed in equation 3.9 in Chapter 3.

Figure 4.9 and Figure 4.10 display the diffusion curves according to the Fick's second law at 10℃, 20℃, and 30℃ in 95% ethanol and their respective residuals plots. The residual plot is used to check whether the assumptions made in the regression analysis are accurate. Based on the Figures 4.9 and 4.10, the residuals plots do not exhibit characteristic signatures and/or patterns, which means that the used regression model is accurate enough.

Table 4.10 $K_{P,S}$ and **α** values of α-TOC and PG for the diffusion from PBAT films into 95% ethanol at 10℃, 20℃, and 30℃ *

Temperature (℃)	$K_{P,S}$		**α**	
	α-TOC	**PG**	**α-TOC**	**PG**
10	0.66±0.02 a	1.18±0.11 b	411.10±14.48	225.02±20.62
20	0.73±0.12 a	1.03±0.47 b	371.30±54.33	212.63±59.64
30	0.73±0.07 a	1.12±0.12 b	388.45±56.85	229.82±26.94

*The data are the averages of four samples ± the standard deviation. Different letters within the same columns indicate statistically significant different values ($p<0.05$)

Table 4.11 *D* and RMSE of α-TOC and PG for the diffusion from PBAT films into 95% ethanol at three different temperature *

Temperature (℃)	**D $\times 10^{-9}$ (cm^2/s)**		**RMSE $\times 10^{-6}$ * (g antiox. /g 95%ethanol)**	
	α-TOC	**PG**	**α-TOC**	**PG**
10	2.05±0.37 a, A	1.86±0.13 a, A	3.54	6.59
20	3.25±0.18 a, B	4.42±0.61 b, B	5.01	0.11
30	7.94±0.71 a, C	8.59±0.12 a, C	9.36	0.14

* The data are the averages of four samples ± the standard deviation. Different lower case letters within the same row indicates statistically significant different values ($p<0.05$). Different upper case letters within the same column indicates statistically significant different values ($p<0.05$). RMSE: root mean square error.

Table 4.12 M_∞ and RMSE of α-TOC and PG for the diffusion from PBAT films into 95% ethanol at three different temperature *

Temperature (℃)	$M_\infty \times 10^{-4}$ (g antiox. /g 95%ethanol)		RMSE $\times 10^{-6}$ * (g antiox. /g 95%ethanol)	
	α-TOC	PG	α-TOC	PG
10	0.71±0.03 a	0.86±0.02 b	3.54	6.59
20	1.08±0.04 a	1.02±0.08 a	5.01	0.11
30	1.02±0.06 a	0.96±0.07 b	9.36	0.14

*The data are the averages of four samples ± the standard deviation. Different letters within the same row indicate statistically significant different values ($p<0.05$). RMSE: root mean square error.

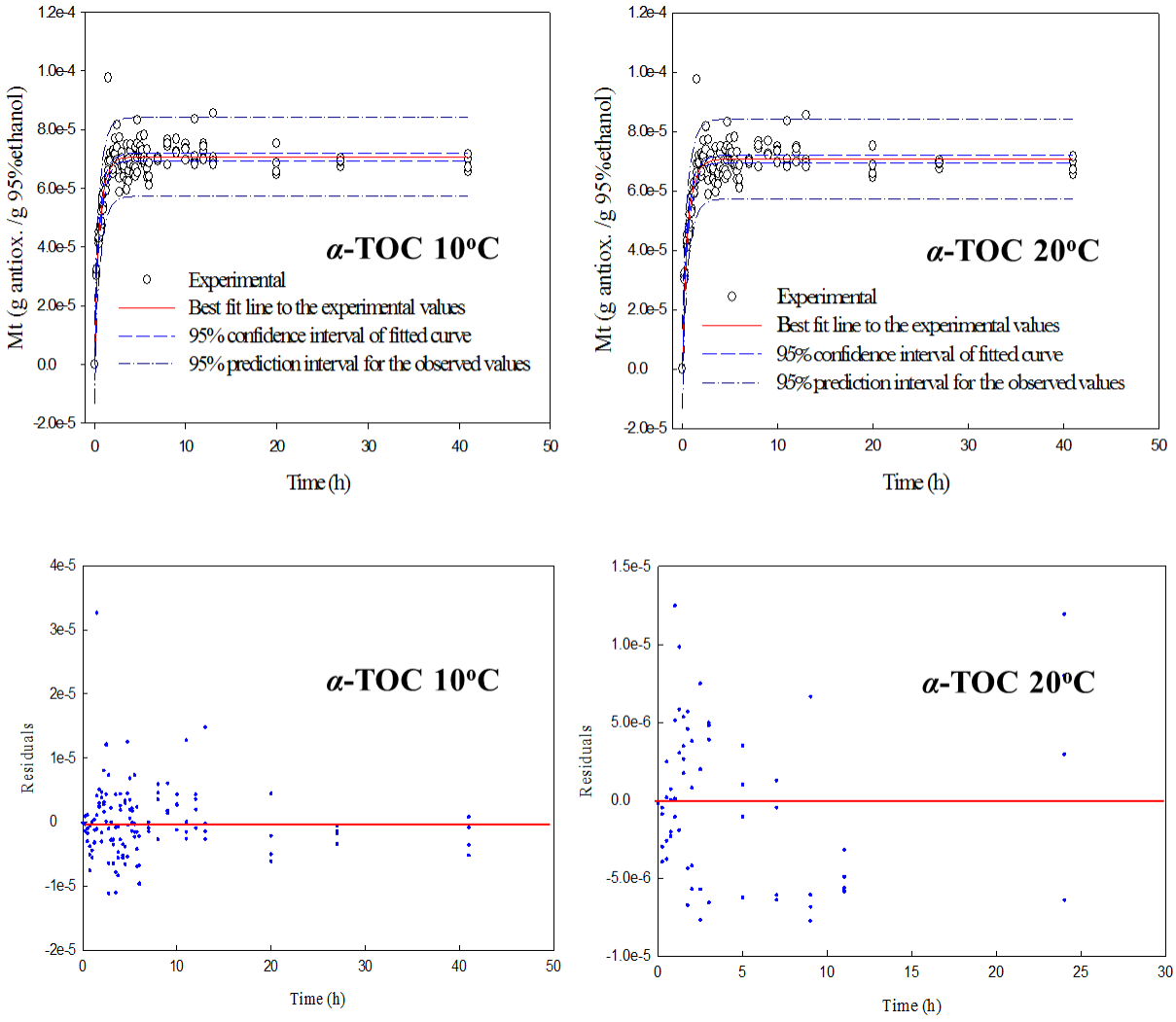

Figure 4.9 Diffusion of α-TOC into 95% ethanol at 10℃ , 20℃ , and 30℃ according to the second Fick's law and their respective residuals plot. The y-axis shows the mass of antioxidants diffused at time t in h.

Figure 4.9 (cont'd)

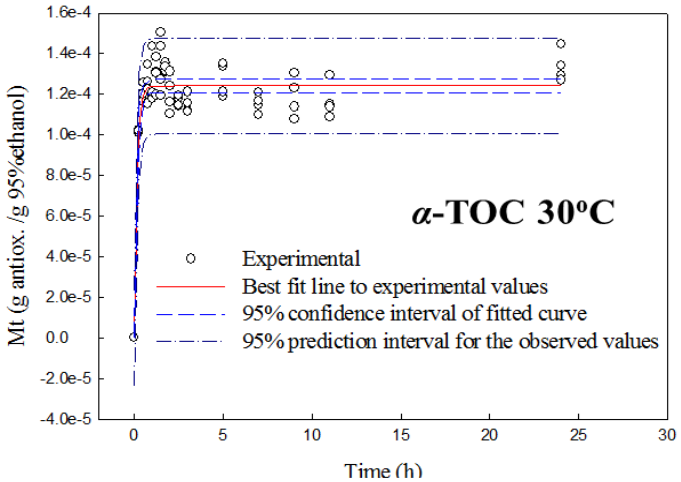

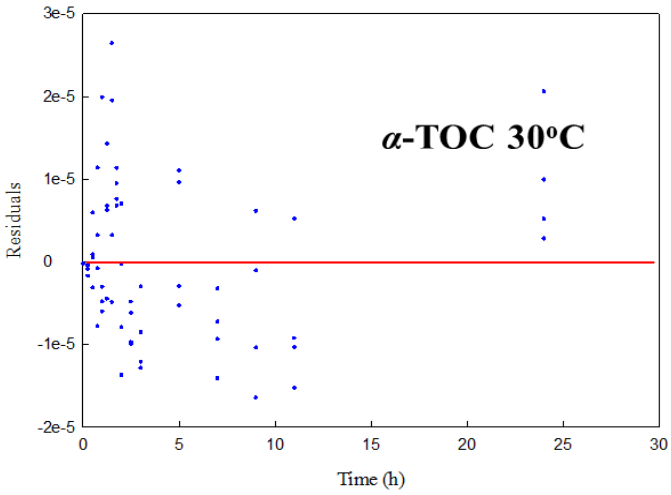

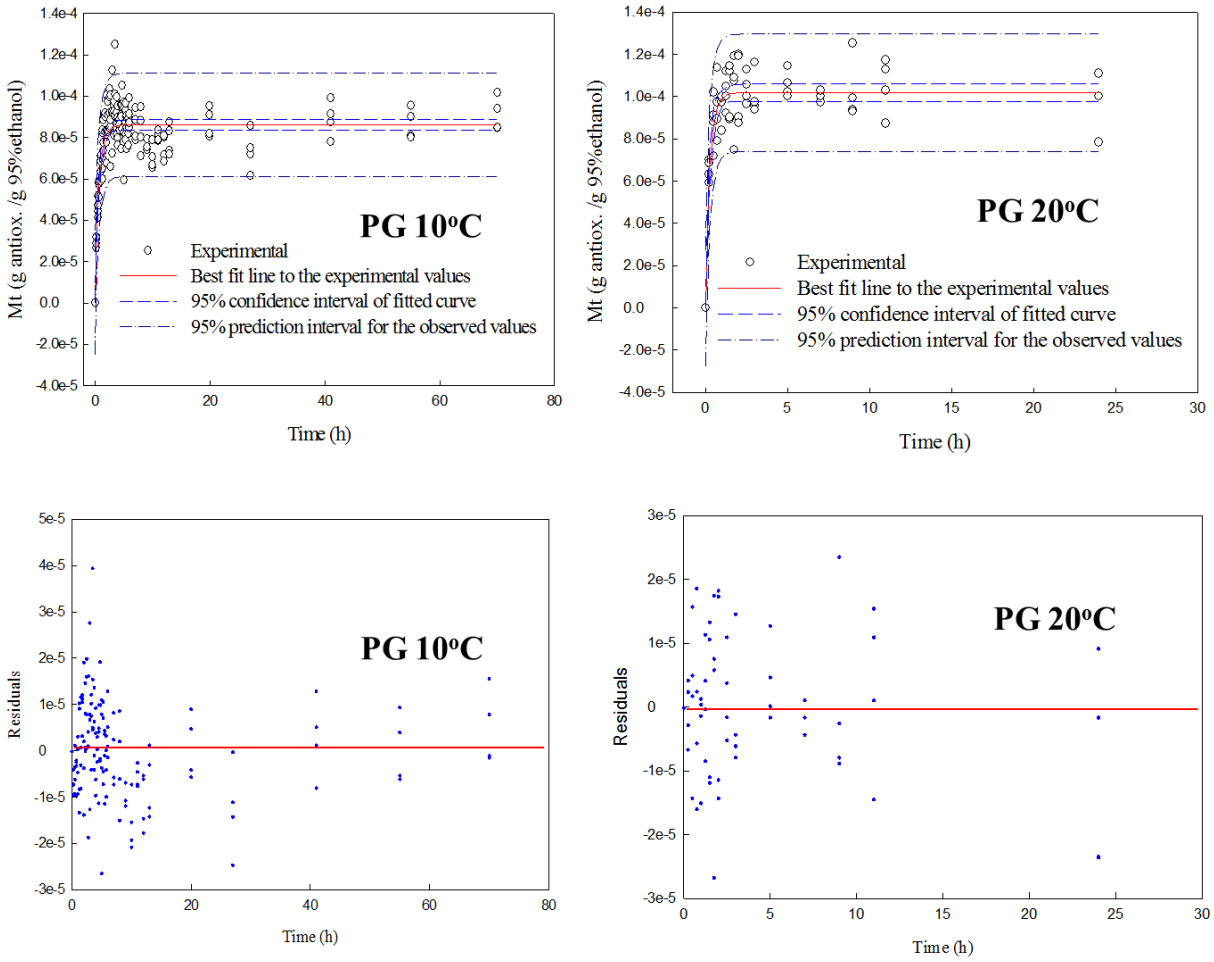

Figure 4.10 Diffusion of PG into 95% ethanol at 10℃ , 20℃, and 30℃ according to the second Fick's law and their respective residuals plot. The y-axis shows the mass of antioxidants diffused at time t in h.

Figure 4.10 (cont'd)

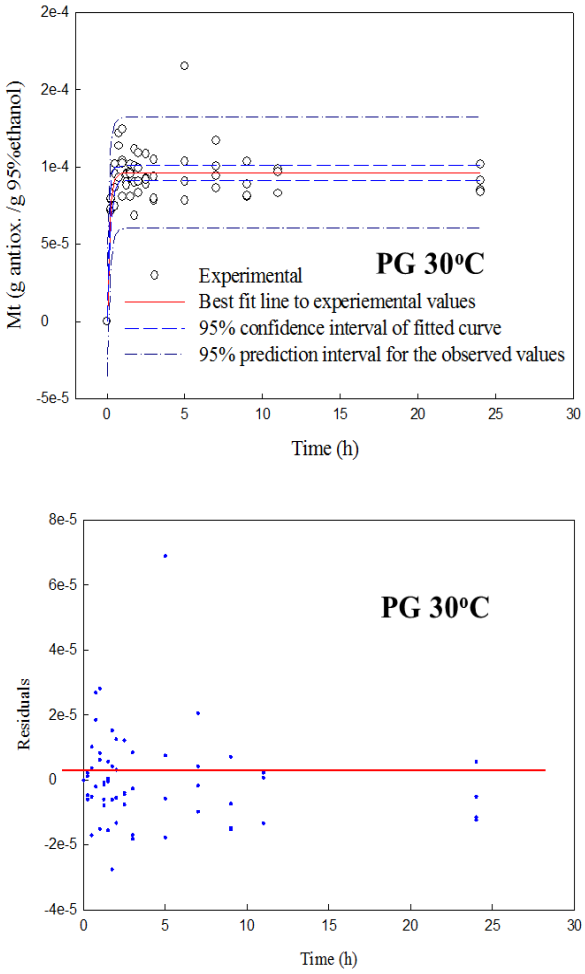

Tables 4.11 and 4.12 show the D and M_∞ values and RMSE values obtained by using equation 3.9, since $K_{P,S} \approx 1$ and $\alpha \gg 1$ for both diffusion of α-TOC and PG. At 10℃, D for α-TOC and PG were 2.05×10^{-9} and 1.86×10^{-9} cm^2/s, respectively. At 20℃, D for α-TOC and PG were 3.25×10^{-9} and 4.42×10^{-9} cm^2/s, respectively. Meanwhile, D values at 30℃ has the same order of magnitude than at 10 and 20℃ , giving values of 7.94×10^{-9} cm^2/s for α-TOC and 8.59×10^{-9} cm^2/s for PG. D values for α-TOC at the three different temperatures were significantly difference from each other and values increase with an increas in temperature. Although D values for α-TOC were different, they were in the same order of magnitude (10^{-9} cm^2/s). Indicating that temperature made a difference on the diffusion process of antioxidants but its

influence was low in this study due to the fast release at all temperatures. The same trend also appeared to *D* values for PG. When comparing the *D* values for α-TOC and PG at each temperature, only at 20℃, they were significantly difference, being the *D* of PG larger than the *D* of α-TOC. In the HSP three-dimension graph, the location of PG is closer to the sphere of ethanol, which should indicate that PG has higher affinity to ethanol than α-TOC. However, at 10 and 30℃, *D* for α-TOC and PG were not significantly different (p-value>0.05). So, indicating that the precision of the HSP may not be sufficient to differentiate the affinity between these antioxidants and ethanol.

Reported *D* values for α-TOC from PLA to ethanol at 23, 33 and 43℃ were 3.16×10^{-11}, 5.29×10^{-11} and 3.8×10^{-10} cm^2/s, respectively[11]. Heirlings et al [17] reported *D* values for α-TOC from polymers like LDPE and ethylene vinyl acetate (EVA) in 95% ethanol at 7℃ as 2.64×10^{-11} and $4.23\times10^{-11}cm^2/s$, respectively. Since there is a little research done on the migration of PG in polymer systems, it is hard to compare the *D* values of PG in other polymer systems. Result from this study shows that *D* values for α-TOC and PG at each temperature were of the same magnitude (10^{-9} cm^2/s), which is faster than that in PLA, LDPE and EVA. Figure 4.5 showed that the location of PBAT in the HSP space is closer to ethanol compared with PLA, which means ethanol has a good solubility to PBAT. So, if we compare ethanol as solvent, ethanol should be better solvent for PBAT than PLA and has more interaction penetrating into the PBAT chains and promote the diffusion of the antioxidants. To the best of the author's knowledge, extensive research of interaction of solvents with PBAT is not found in the peer-review literature. Based on equation 3.1, the distance R_a between α-TOC and PBAT is 8.0 and the distance R_a between PG and PBAT is 10.8. The distance of these two antioxidants to PBAT is not quite different. Even though based on Figure 4.6 PG is closer to ethanol, the similar

distance to PBAT and the aggressive ethanol solvent could contribute to the similar diffusion process of α-TOC and PG obtained in this study. Even at 10℃ the diffusion of α-TOC and PG were very fast and there was not a significant difference between them. So, it is understandable that the diffusion difference between α-TOC and PG at 30℃ is not significantly different since the values are so high to start. Further studies are needed to understand if the estimation of the HSP can be useful to predict chemical compounds, polymers and solvents compatibilities, and to determine if proper estimation can be achieved for different molecules with different functional groups and basic chemical structures.

4.6 Activation energy (*Ea*) of the diffusion of selected antioxidants into 95% ethanol

The Arrhenius equation was used to determine the *Ea* of α-TOC and PG into 95% ethanol. The Ea can be defined as the energy required for an additive molecule to move through the polymer matrix [18]. Figure 4.11 shows the Arrhenius plots of α-TOC and PG from PBA and PBP films, respectively. The plot of Log D versus 1/T gave a linear line with an Ea of 48.5 ± 8.8 kJ/mol for PBA, 54.2 ± 6.9 kJ/mol for PBP. The Ea values of α-TOC and PG are not statistically significant difference ($p>0.05$).

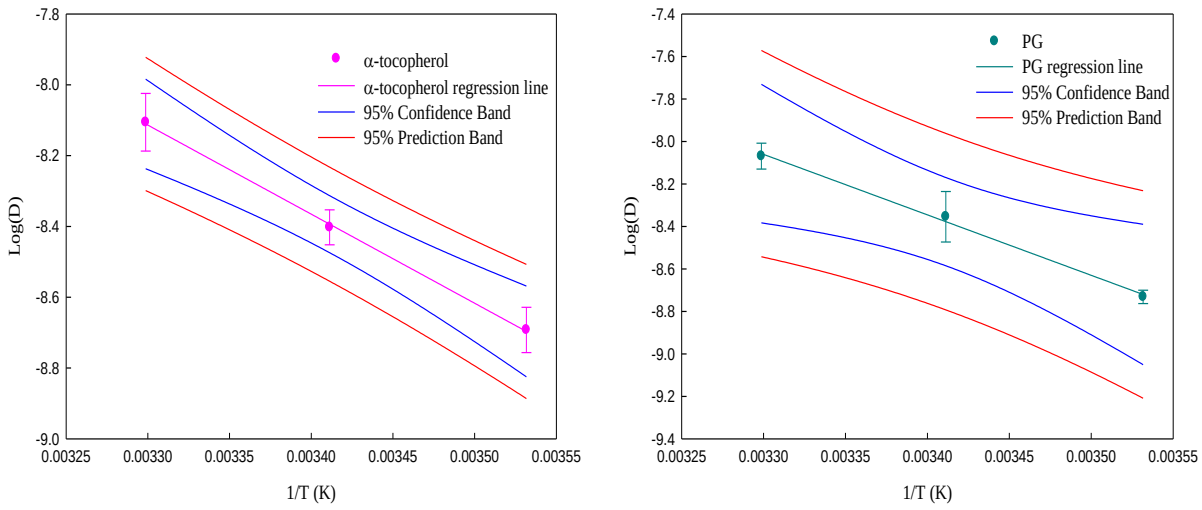

Figure 4.8 The activation energy for diffusion of α-TOC (y= -2515.8649+0.1886; R^2=0.9450) (in the left side of Figure) and PG (y= -2859.4411x+1.4215; R^2=0.9211) (in the right side of Figure) from processed film into 95% ethanol. The slope of each line was equal to –Ea/2.03R.

The *Ea* values reported for α-TOC diffusion from PLA to ethanol was 96.2 kJ/mol [11] and for α-TOC diffusion from a multilayer active packaging (made of HDPE, eEVA and a layer of LDPE containing the antioxidant) to whole milk powder was 11.3 kJ/mol [19], so it can be observed that α-TOC in different polymer systems have large differences. This difference could be mainly attributed to the nature of PBAT being a flexible polymer and mostly amorphous which allows a fast release of α-TOC from its chains. No diffusion of PG in polymer has been reported, so the comparison of PG in different polymer cannot be made. In this study, the relative low *Ea* for α-TOC and PG can be interpreted as the low energy required for these two antioxidants to diffuse from the processed films into 95% ethanol at temperatures from 10 to 30℃.

4.7 Optical property

PBC film presents a milky color. PBA film displays a beige color with varying intensities, while PBP film shows an obvious orange color (Figure 4.12). Table 4.14 shows the *CIE L*a*b* values for these three different films.

Figure 4.9 The appearance of PBC (left), PBA (middle), PBP (right)

Table 4.13 CIE L*a*b values and total color change (**ΔE**) for PBC, PBA, PBP [*]

Film	L*	a*	b*	ΔE [1]
PBC	93.57±0.06 [a]	-1.19±0.03 [b]	0.61±0.04 [c]	-
PBA	92.31±0.02 [b]	-1.07±0.03 [b]	5.37±0.25 [b]	4.93
PBP	87.28±0.06 [c]	1.62±0.08 [a]	21.92±0.30 [a]	22.40

[*] PBC was used as a reference. Results are means ± the standard deviation of three replicates. Different letters within the same columns indicate statistically significant different values ($p<0.05$)

[1] $\Delta E = \sqrt{\Delta L^2 + \Delta a^2 + \Delta b^2}$.

According to table 4.14, the addition of α-TOC and PG did affect the lightness (*L**) ($p<0.05$) and yellowness (*b**) ($p<0.05$) of the films. A minor difference of *L** were found between PBC and PBP, while PBP has the lowest *L** compared to PBC and PBA. PBP has the highest *b** value compared to other two films. The greenness (*a**) of PBC and PBA were not significantly different, while the greenness (*a**) of PBP was higher than PBC and PBA. The total difference in color ΔE for PBA was 4.93 and for PBP was 22.40. PBP film has a bigger color change, which can be seen by its orange color (Figure 4.12). PBA also shows color change, it is

barely perceptible to the eye in the single film layer but the color was perceptible in the film rolls to the naked eye.

Figure 4.13 shows the UV-visible light transmission spectra of PBC, PBA and PBP films. The three films exhibited nearly no light transmission from 300 to 200nm. There is a slight difference between PBC and PBA from 300 to 500nm, and the difference is more obvious between PBC and PBP from 300 to 500 nm, which is due to the color changes in the film and the absorption of the functional group C=O and –OH [20].

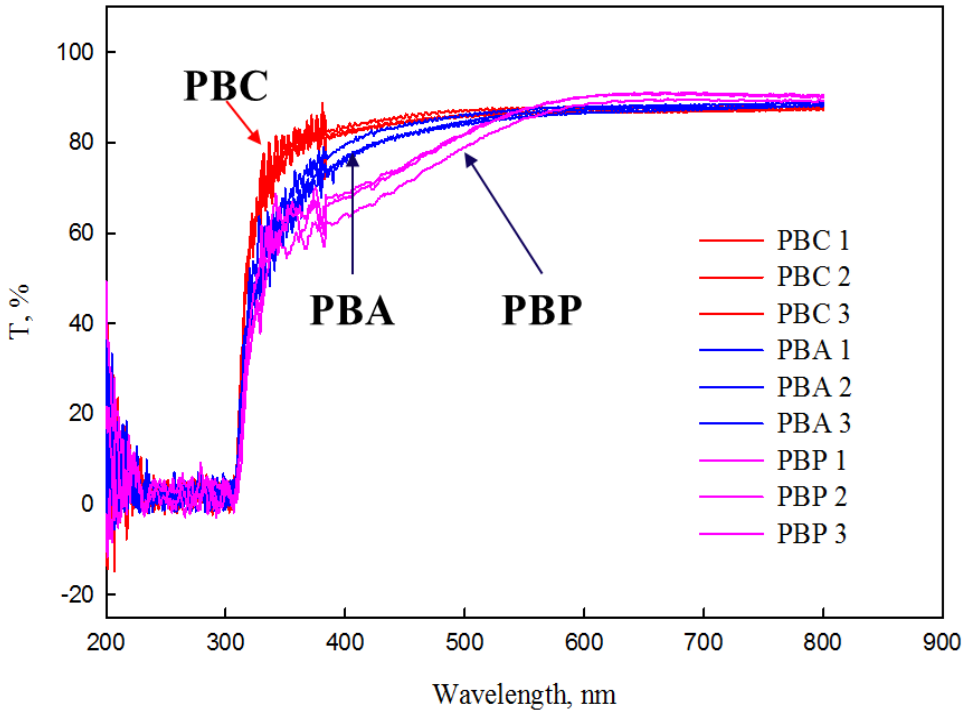

Figure 4.10 UV-visible light transmission spectra of PBC, PBA and PBP films. The film thicknesses of PBC, PBA and PBP were 63.5 ± 5.1, 68.6 ± 2.5 and 76.2 ± 5.1**µm**, respectively.

REFERENCES

REFERENCES

1. Hansen, C.M., *Hansen solubility parameters: a user's handbook*. 2007: CRC.

2. Auras, R.A., et al., *Poly (lactic acid): synthesis, structures, properties, processing, and applications*. Vol. 10. 2011: Wiley.

3. Van Krevelen, D. and K. Nijenhuis, *Properties of polymers. Their correlation with chemical structure: their numerical estimation and prediction from additive groups contributions.* Elsevier, New York, 1990.

4. Ortiz-Vazquez, H., et al., *Release of butylated hydroxytoluene (BHT) from Poly (lactic acid) films.* Polymer Testing, 2011. **30**(5): p. 463-471.

5. Sharma, O.P. and T.K. Bhat, *DPPH antioxidant assay revisited.* Food Chemistry, 2009. **113**(4): p. 1202-1205.

6. Al-Malaika, S., H. Ashley, and S. Issenhuth, *The antioxidant role of α-tocopherol in polymers. I. The nature of transformation products of α-tocopherol formed during melt processing of LDPE.* Journal of Polymer Science Part A: Polymer Chemistry, 1994. **32**(16): p. 3099-3113.

7. Reda, S.Y., *Evaluation of antioxidants stability by thermal analysis and its protective effect in heated edible vegetable oil.* Ciência e Tecnologia de Alimentos, 2011. **31**(2): p. 475-480.

8. chemicals, C.s., *Ciba® IRGANOX® 1076.* Ciba® product introduaction, 2004.

9. Soto-Cantú, C., et al., *Release of butylated hydroxytoluene from an active film packaging to asadero cheese and its effect on oxidation and odor stability.* Journal of dairy science, 2008. **91**(1): p. 11-19.

10. Graciano-Verdugo, A.Z., et al., *Migration of α-tocopherol from LDPE films to corn oil and its effect on the oxidative stability.* Food research international, 2010. **43**(4): p. 1073-1078.

11. Manzanarez-López, F., et al., *Release of α-Tocopherol from Poly (lactic acid) films, and its effect on the oxidative stability of soybean oil.* Journal of Food Engineering, 2011. **104**(4): p. 508-517.

12. Samsudin, H., et al. *Application of Parameter Estimation to Predict Migration of Antioxidant Films*. in *6th Shelf Life International Meeting*. 2014. New Brunswick, NJ.

13. Dolan, K.D. and D.K. Mishra, *Parameter Estimation in Food Science.* Annual review of food science and technology, 2013. **4**: p. 401-422.

14. Tehrany*, E. and S. Desobry, *Partition coefficients in food/packaging systems: a review.* Food additives and contaminants, 2004. **21**(12): p. 1186-1202.

15. Limm, W. and H.C. Hollifield, *Modelling of additive diffusion in polyolefins.* Food Additives & Contaminants, 1996. **13**(8): p. 949-967.

16. Crank, J., *The mathematics of diffusion*. 1979: Oxford university press.

17. Heirlings, L., et al., *Influence of polymer matrix and adsorption onto silica materials on the migration of α-tocopherol into 95% ethanol from active packaging.* Food additives and contaminants, 2004. **21**(11): p. 1125-1136.

18. Iñiguez-Franco, F., et al., *Antioxidant Activity and Diffusion of Catechin and Epicatechin from Antioxidant Active Films Made of Poly (l-lactic acid).* Journal of agricultural and food chemistry, 2012. **60**(26): p. 6515-6523.

19. Granda-Restrepo, D.M., et al., *Migration of α-tocopherol from an active multilayer film into whole milk powder.* Food research international, 2009. **42**(10): p. 1396-1402.

20. Hong, X., et al., *Visible-light-activated nanoparticle photocatalyst of iodine-doped titanium dioxide.* Chemistry of Materials, 2005. **17**(6): p. 1548-1552.

CHAPTER 5 CONCLUSIONS

This study explored the use of the Hansen Solubility Parameters (HSP) methodology to estimate the affinity between polymer and antioxidants (AOxs) in AOx packaging films (APF), in order to understand the control release of AOx in different packaging systems. Poly (butylene adipate-*co*-terephthalate) (PBAT) was targeted as studied biodegradable polymer, and twenty-five commonly used AOxs were considered as candidates. The HSPs of PBAT were measured by an experimental method and the Hoftyzer and Van-Krevelen theoretical calculation method. The values from both methods were found similar. The data from the experimental method was used to conduct this work, which were 18.97, 4.83 and 9.10 for the δ_d, δ_p and δ_h,respectively. The HSPs of selected AOxs were also calculated based on the Hoftyzer and Van-Krevelen method. After determining and plotting the HSPs of PBAT ethanol (a food simulant) and selected AOxs in a 3D plot, propyl gallate (PG) and α-tocopherol (α-TOC) were chosen to incorporate in PBAT. According to the basic principle of HSP, the greater distance between the HSP of the two materials, the less alike they are. So, PG is closer located in the region of interaction of ethanol and α-TOC is closer located in the region of interaction of PBAT. So, migration test in 95% ethanol were conducted for these antioxidants-PBAT films to verify if the HSP estimation that α-TOC incorporated in PBAT will have less affinity towards ethanol than PG.

In order to conduct the migration test, two PBAT films added with α-TOC and PG were produced (2% PG-PBAT (PBP) and 2% α-TOC-PBAT (PBA).) The final concentration of antioxidants in the films were 1.8% (w/w) for PBP and 1.5% (w/w) for PBA due to the adherence of antioxidants to the screw and the barrel. Preliminary migration study was performed to determine the optimal experimental design for the migration test for these two films. Based on the scaled sensitivity coefficient (SSC) analysis during the preliminary migration study, the final

migration tests were conducted at 10, 20 and 30℃ for the produced films. The diffusion of both antioxidants into 95% ethanol followed Fick's law for diffusion. The equilibrium at 10℃, 20℃ and 30℃ for both PBP and PBA films was obtained at 1.75 h, 1h and 0.75 h, respectively. At the end of the migration study, more than 99% of α-TOC and PG was migrated from PBA film into 95% ethanol. Parameters related to migration process such as diffusion coefficients (*D*) and partition coefficients ($K_{P,S}$) were determined by solving the Fick's diffusion equations. $K_{P,S}$ for α-TOC at three temperatures were all less than 1, while $K_{P,S}$ for PG at all temperature were slightly above 1. The low $K_{P,S}$ for both α-TOC and PG agreed with the release of more than 99% AOxs into 95% ethanol. *D* values for α-TOC and PG increase with the increasing temperature, which means that temperature made a difference on the diffusion process. However, D values for both PBA and PBP films at all three temperatures were in the same order of magnitude (10^{-9} cm^2/s) due to the fast release at all temperatures. When comparing the *D* values between α-TOC and PG at each temperature, only at 20℃ there was a significantly different between them. *D* of PG was larger than *D* of α-TOC. The difference was not found at 10℃ and 30℃, indicating that the HSP may not estimate the affinity between the antioxidants and ethanol due to the fast release of these compounds from this polymer. The activation energy (*Ea*) of α-TOC and PG were calculated by Arrhenius equation, resulting as 48.5 kJ/mol for the release of α-TOC from PBAT and 54.2 kJ/mol for the release of PG from PBAT.

There were obvious changes on the optical properties of PBA and PBP compared with the PBAT control (PBC) film. PBA films display a beige color while PBP display a heavy orange color. The transmission spectra of UV visible light of PBC, PBA and PBP films also presented difference on the light transmission from 300 to 500 nm, due to the color changes in the film and the functional groups of the AOxs.

5.1 Future work

According to the outcomes obtained from this study, the future work may concentrate on the followings:

1) To determine if the HSP can be used to estimate the affinity between PBAT and AOxs that are further located in the Hansen solubility parameter space.
2) To use other solvents to investigate the release of these antioxidants such as water and oil.
3) To determine the limitation of the HSP to estimate the affinity between polymer and AOxs.
4) To further understand the use of prediction methods to determine the affinity between polymers and different chemical compounds.